Assignment of the Optical Spectra of Metal Phthalocyanine Anions

John Mack and Martin J. Stillman*

Department of Chemistry, University of Western Ontario, London, Ontario, Canada N6A 5B7

Received June 20, 1996[⊗]

Specially designed spectroelectrochemical cells were used to record UV−vis absorption and magnetic circular dichroism (MCD) spectral data of the phthalocyanine ring-reduced dianion, $[ZnPc(-4)]^{2-}$, *in situ* at room temperature. $[ZnPc(-4)]^{2-}$ was generated at cryogenic temperatures through photoreduction of a vitrified dimethyl formamide/hydrazine hydrate solution using hydrazine as the electron donor. Molecular orbital calculations for $[ZnPc(-(2 + n))]^{-n}$ ($n = -1-4$) species were performed through the use of the ZINDO program. The approach that was developed previously to assign the major $\pi \rightarrow \pi^*$ and $\pi^* \rightarrow \pi^*$ transitions in the optical spectrum of $[ZnPc(-3)]^-$, which was based on analysis of the relative signs and intensities of close lying Faraday B terms in the MCD spectrum, is used here to assign the major bands seen in the spectrum of $[ZnPc(-4)]^{2-}$. The spectrum is dominated by a $\pi^* \rightarrow \pi^*$ transition out of the partially filled lowest unoccupied molecular orbital (LUMO) which gives rise to a pair of oppositely-signed, coupled B terms in the MCD spectrum at 506 and 620 nm. The Q transition of the phthalocyanine ring is assigned to a weak absorption band at 865 nm, while the second $\pi \rightarrow \pi^*$ transition is assigned to a band at 370 nm. The band assignment scheme is extended to data that have been reported previously for more highly ring-reduced main group $[MPc(-5)]^{3-}$ and $[MPc(-6)]^{4-}$ species (M = Mg, Zn). The Q band of $[MgPc(-5)]^{3-}$ is assigned to a band at 1125 nm. Bands at 589 and 825 nm are assigned to $\pi^* \rightarrow \pi^*$ transitions out of the partially occupied Jahn−Teller split e_g^* LUMO. The second $\pi \rightarrow \pi^*$ transition is assigned to a band at 338 nm. As the LUMO is fully occupied, the spectrum of $[MgPc(-6)]^{4-}$ is dominated by $\pi^* \rightarrow \pi^*$ bands at 625 and 840 nm. An additional band at 305 nm is assigned to the second $\pi \rightarrow \pi^*$ transition. A general band assignment scheme is proposed for both main group and transition metal phthalocyanine anion species.

Introduction

Metal porphyrin complexes play a vital role in biological processes such as photosynthesis and respiration.[1] These complexes offer a unique chemistry that has a great many possible industrial applications. Perhaps the most commercially important group of the porphyrin class of molecules is the phthalocyanines, known systematically as the tetraazatetrabenzoporphyrins.[2] The phthalocyanine ring contains a heteroaromatic π-system, Figure 1. Electrochemical studies have shown that up to four electrons can be reversibly added to, or up to two reversibly removed from, the π-system of the phthalocyanine dianion ring. A number of research groups have used spectroelectrochemical cells to record spectra of the $[MPc(-3)]^-$ and $[MPc(-4)]^{2-}$ species of a number of phthalocyanines.[3−10] Clack and Yandle reported the band maxima and relative intensities of a wide range of $[MPc(-(2 + n))]^{n-}$ ($n = 1-4$) species that were generated chemically *in vacuo* over sodium films.[3] Linder *et al.* used this technique to record room temperature absorption and magnetic circular dichroism (MCD) spectral data for the four reduced species of MgPc.[11] However, no band assignments have been attempted in any of these papers. Minor *et al.*[12] have proposed a general assignment of the bands in the absorption spectra of the cationic and anionic species of a number of different metal phthalocyanine complexes based upon the spectral data that was then available in the literature. Analysis of the low-temperature MCD spectra of $[ZnPc(-3)]^-$ that we recently reported[13] provided a complete assignment of the optical spectrum of main group ring-reduced $[MPc(-3)]^-$ species. In this present paper, an assignment scheme is proposed that fully accounts for the features observed in the currently available optical spectral data of $[MPc(-3)]^-$, $[MPc(-4)]^{2-}$, $[MPc(-5)]^{3-}$, and $[MPc(-6)]^{4-}$ species based, in particular, on an analysis of the MCD data.

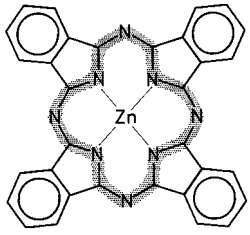

Figure 1. Molecular structure of zinc phthalocyanine showing the path of the 16-membered polyene ring that was used as the basis for the four-orbital LCAO calculations of Gouterman that were used to account for the two lowest energy transitions in porphyrins and phthalocyanines.[14]

* To whom correspondence should be addressed. Fax: (519) 661-3022. Tel: (519) 661-3821. Internet: Stillman@uwo.ca.

⊗ Abstract published in *Advance ACS Abstracts,* January 1, 1997.

(1) (a)*The Porphyrins*; Dolphin, D., Ed.; Academic Press: New York, 1978. (b) *Ann. NY Acad. Sci.* **1973**, 206.
(2) *Phthalocyanine. Principles and Properties*; Leznoff, C. C., Lever, A. B. P., Eds.; VCH Publications: New York, 1989; Vol. I. (b) *Phthalocyanine. Principles and Properties*; Leznoff, C. C., Lever, A. B. P., Eds.; VCH Publications: New York, 1993; Vol. II. (c) *Phthalocyanine. Principles and Properties*; Leznoff, C. C., Lever, A. B. P., Eds.; VCH Publications: New York, 1993; Vol. III.
(3) Clack, D. W.; Yandle, J. R. *Inorg. Chem.* **1972**, *11*, 1738.
(4) Rollman, L. D.; Iwamoto, R. T. *J. Am. Chem. Soc.* **1968**, *90*, 1455.
(5) Nevin, W. A.; Hempstead, M. R.; Liu, W.; Leznoff, C. C.; Lever, A. B. P. *Inorg. Chem.* **1987**, *26*, 570.
(6) Nevin, W. A.; Liu, W.; Greenberg, S.; Hempstead, M. R.; Marcuccio, S. M.; Melnik, M.; Leznoff, C. C.; Lever A. B. P. *Inorg. Chem.* **1987**, *26*, 891.
(7) Louati, A.; El Meray, M.; Andre, J. J.; Simon, J.; Kadish, K. M.; Gross, M.; Giraudeau A. *Inorg. Chem.* **1985**, *24*, 1175.
(8) Giraudeau, A.; Louati, A.; Gross, M.; Andre, J. J.; Simon, J.; Su, C. H.; Kadish, K. M. *J. Am. Chem. Soc.* **1983**, *105*, 1175.
(9) Golovin, N. M.; Seymour, P.; Jayaraj, K.; Fu, Y.; Lever, A. B. P. *Inorg. Chem.* **1990**, *29*, 1719.
(10) Lever, A. B. P.; Wilshire, J. P. *Inorg. Chem.* **1978**, *17*, 1145.
(11) Linder, R. E.; Rowland, N. S.; Hush, N. S. *Mol. Phys.* **1971**, *21*, 417.
(12) Minor, P. C.; Gouterman, M.; Lever, A. B. P. *Inorg. Chem.* **1985**, *24*, 1894.
(13) Mack, J.; Stillman, M. J. *J. Am. Chem. Soc.* **1994**, *116*, 1292.

S0020-1669(96)00737-9 CCC: $14.00

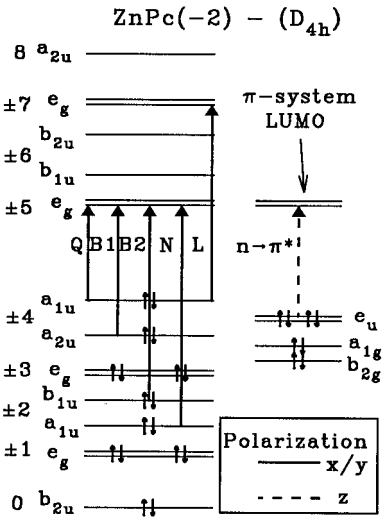

Figure 2. Molecular orbital diagram of ZnPc(−2) showing the transitions that are predicted to give rise to absorption bands in the 250−1000 nm range on the basis of Gouterman's SCMO-PPP-CI model[17] and spectral deconvolution studies.[18,24] The orbital ordering on the left is based on Gouterman's Hückel treatment model of the inner ring cyclic polyene.[14] The orbitals on the right are the four aza-nitrogen lone pair orbitals. Transitions that give rise to *x*/*y*-polarized bands are represented with solid lines. Dashed lines are used for *z*-polarized transitions.

Gouterman's four-orbital model has been widely used to describe the optical spectra of both metal porphyrin and metal phthalocyanine complexes.[14−18] Gouterman's model is based on a theoretical treatment that unites a 16 atom, 18 π-electron cyclic polyene model with a Hückel treatment that takes into account the structure of the porphyrin ring. The molecular orbital diagram shown in Figure 2 is derived from this simple cyclic polyene model.[14,19,20] The association of the orbital angular momentum (OAM) with pairs of orbitals follows from the assignment of the molecular orbitals of an aromatic ring in terms of the OAM that is associated with the complex wave functions of an ideal cyclic polyene in the sequence 0, ±1, ±2, ..., ±7, 8. The highest occupied molecular orbital (HOMO) has an M_L value of ±4 while the lowest unoccupied molecular orbital (LUMO) has an M_L value of ±5. In this simple scheme, there are four transitions between these two levels involving changes in orbital angular momentum of $\Delta M_L = \pm 1$ and ±9, Figure 2. Despite the obvious simplicity of this model, it provides a remarkably good description of the experimental spectral data of main group metal porphyrin complexes.[14]

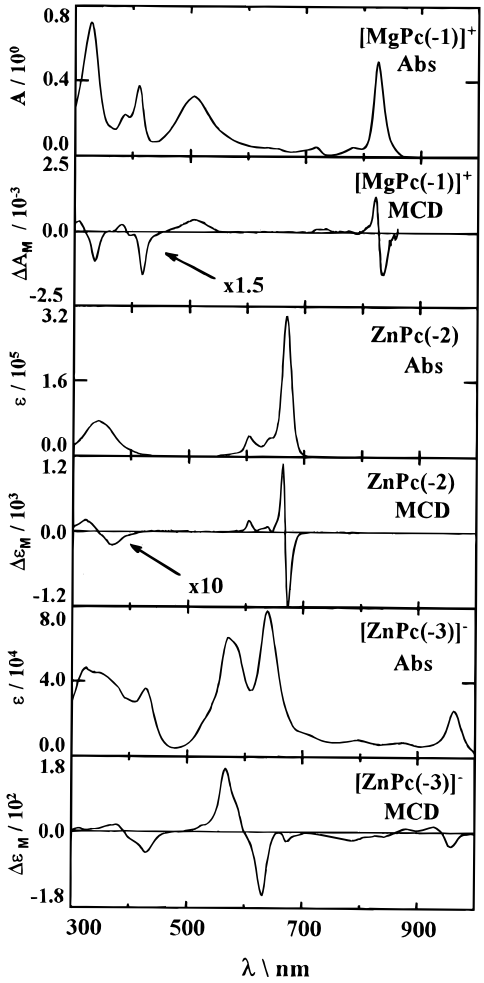

Figure 3. Absorption and MCD spectra for $[MgPc(-1)]^+$ in CH_2Cl_2,[24] ZnPc(−2) in DMF, and $[ZnPc(-3)]^-$ in DMF/hydrazine hydrate.[13] None of the MCD bands observed for $[ZnPc(-3)]^-$ can be fitted with A terms such as that seen for the Q band of ZnPc(−2) at 670 nm.

The addition of the aza-linkages and fused benzenes to form the phthalocyanine molecule breaks the accidental degeneracy of the a_{1u} and a_{2u} orbitals significantly. This results in mixing between the excited states so that the previously forbidden Q transition gains significant intensity from the allowed B transition, Figure 3, and is observed as an intense band near 670 nm.[14a] Gouterman's model of the electronic structure has been used as the theoretical framework within which to assign specific $\pi \rightarrow \pi^*$ transitions in MPc(−2) and MP(−2) complexes and their cation radicals. We have used spectral deconvolution calculations on the UV−vis absorption and MCD spectra,[21] using the program SIMPFIT, to provide the polarization and energies for these bands.[18,22−25] These studies[18,22−25] have

(14) (a) Gouterman, M. In *The Porphyrins*; Dolphin, D., Ed.; Academic Press: New York, 1978; Vol. III, Part A, pp 1−165. (b) Gouterman, M. *J. Mol. Spectrosc.* **1972**, *44*, 37. (c) Gouterman, M.; Wagniere, G. H.; Snyder, L. C. *J. Mol. Spectrosc.* **1963**, *11*, 108.
(15) (a) Michl, J. *J. Am. Chem. Soc.* **1978**, *100*, 6801. (b) Michl, J. *Pure Appl. Chem.* **1980**, *52*, 1549.
(16) Weiss, C.; Kobayashi, H.; Gouterman, M. *J. Mol. Spectrosc.* **1965**, *16*, 415.
(17) McHugh, A. J.; Gouterman, M.; Weiss, C. *Theor. Chim. Acta* **1972**, *24*, 346.
(18) (a) Nyokong, T.; Gasyna, Z.; Stillman, M. J. *Inorg. Chem.* **1987**, *26*, 1087. (b) Stillman, M. J.; Nyokong, T. N. In *Phthalocyanine. Principles and Properties*; Leznoff, C. C., Lever A. B. P., Eds.; VCH Publications: New York, 1989; Vol. I, Chapter 3, pp 133−289. (c) Stillman, M. J. In *Phthalocyanine. Principles and Properties*; Leznoff, C. C., Lever A. B. P., Eds.; VCH Publications: New York, 1993; Vol. III, Chapter 5, pp 227−296. (d) Ough, E. A.; Stillman, M. J. *Inorg. Chem.* **1994**, *33*, 573. (e) Mack, J. Ph.D. Thesis, University of Western Ontario, 1994.
(19) Perrin, M. H. *J. Phys. Chem.* **1973**, *59*, 2090.
(20) (a) Moffitt, W. *J. Chem. Phys.* **1954**, *22*, 320. (b) Moffitt, W. *J. Chem. Phys.* **1954**, *22*, 1820.
(21) The MCD signal arises from the same transitions as those seen in the UV−vis absorption spectrum, but the selection rules are different as the intensity mechanism depends upon the magnetic dipole moment in addition to the electric dipole moment which normally determines UV−vis absorption intensity.[51] MCD spectroscopy is therefore complementary to UV−vis absorption spectroscopy as it can provide ground and excited state degeneracy information essential in understanding the electronic structure of molecules of high symmetry. The specificity of the MCD technique arises from three highly characteristic spectral features, the Faraday A, B, and C terms.[51] The derivative-shaped Faraday A term is temperature independent and identifies degenerate excited states, while the normally Gaussian-shaped C term is highly temperature dependent and identifies an orbitally degenerate ground state. Gaussian-shaped, temperature independent B terms arise from mixing between closely related states linked by a magnetic dipole transition moment.
(22) Nyokong, T.; Gasyna, Z.; Stillman, M. J. *Inorg. Chem.* **1987**, *26*, 548.

indicated that there are in fact two A terms in the B region of the spectrum of MPc(−2) complexes. Gouterman's model was therefore modified to include separate B1 and B2 transitions that were superimposed in the 350 nm region.[18b] Recently, the major transitions in the optical spectrum of $[ZnPc(-3)]^-$ have been assigned through a spectral band deconvolution analysis of absorption and MCD data recorded at cryogenic temperatures.[13] Cory *et al.*[26] have also reported band assignments for MgPc(−2) and $[MgPc(-3)]^-$ based upon *ab initio* and INDO calculations. In this present paper, new MCD spectral data for the ring-reduced $[ZnPc(-4)]^{2-}$ species are described. The band assignment that was developed for $[ZnPc(-3)]^-$ is extended to the optical spectra of $[MPc(-3)]^-$, $[MPc(-4)]^{2-}$, $[MPc(-5)]^{3-}$, and $[MPc(-6)]^{4-}$ species of a number of different metals on the basis of the available spectral data and the calculations that were performed for the $[MPc(-(2+n))]^{n-}$ ($n = -1-4$) species using the ZINDO program.[27] A general band assignment scheme is proposed for reduced metal phthalocyanine anion species.

Experimental Section

ZnPc (Eastman Kodak) was used as supplied. ZnPc was analyzed by mass spectrometry and gave the expected isotope pattern. Spectrograde dimethylformamide (DMF) was obtained from Omnisolv, and piperidine and hydrazine hydrate were obtained from BDH and used as supplied. Electrochemical reduction was carried out under the control of a PAR model 273 galvanostat/potentiostat. A specially designed spectroelectrochemical cell was used to record UV−vis absorption and MCD spectra as the $[MPc(-4)]^{2-}$ species was being generated *in situ*. These cells were previously used to generate the $[MgPc(-3)]^-$ and $[MgPc(-4)]^{2-}$ species for spectroscopic analyses in which isosbestic spectral changes linked the formation of the Pc(−2), Pc(−3), and Pc(−4) species.[18c,e,28] We have observed that the $[MPc(-4)]^{2-}$ species is most easily formed by applying a fixed potential of greater than 1.5 V in the presence of excess piperidine as an axial ligand. Piperidine can also be used as a donor molecule to aid in the photoassisted reduction of metal phthalocyanine complexes.[29] Both photochemical and electrochemical reduction can, therefore, take place during the *in situ* reduction. Low-temperature $[ZnPc(-4)]^{2-}$ absorption data were recorded in an Oxford Instruments model 204 optical cryostat from a vitrified DMF/hydrazine hydrate (5:2 v/v) solution. The photoreduction was carried out through irradiation with a 300 W tungsten−halogen Kodak projector lamp using a Pyrex filter. A 20% $[ZnPc(-3)]^-$ impurity was subtracted out digitally by assuming that there is negligible absorption by ZnPc(−2) and $[ZnPc(-4)]^{2-}$ at 956 nm, the band center of the most intense $[ZnPc(-3)]^-$ Q band.

Absorption spectra were recorded with an AVIV 17DS spectrophotometer (a spectrometer based on the Cary 17 monochromator). The wavelength accuracy was tested with a holmium oxide filter and was found to be accurate to within ±0.4 nm for 14 peaks between 240 and 650 nm. The photometric accuracy was tested using National Bureau of Standards Neutral Density Schott Filters and was found to be better than 0.1% at 0.3, 0.5, 1.0, 1.5, and 2.0 absorption units. The MCD spectra were recorded on a Jasco J-500C spectrometer with a field of 5.5 T from an Oxford Instruments SM2 superconducting magnet for room temperature data. MCD spectra were recorded digitally under the control of an upgraded version of the program CDSCAN[30,31] on an IBM 9000 series computer. The field strength and sign were calibrated by measuring the MCD spectrum of an aqueous solution of $CoSO_4$ at 510 nm. $[\theta]_M$ was calculated for this instrument to be −59.3 $deg \cdot cm^2 \cdot dmol^{-1} \cdot T^{-1}$. The signal intensity of the CD spectrometer was also tested using ammonium d-camphor-10-sulfonate by ensuring that the $\theta°/A$ ratio for the peaks at 280 nm was 2.26.[32] Base lines were subtracted using SPECTRA MANAGER.[33]

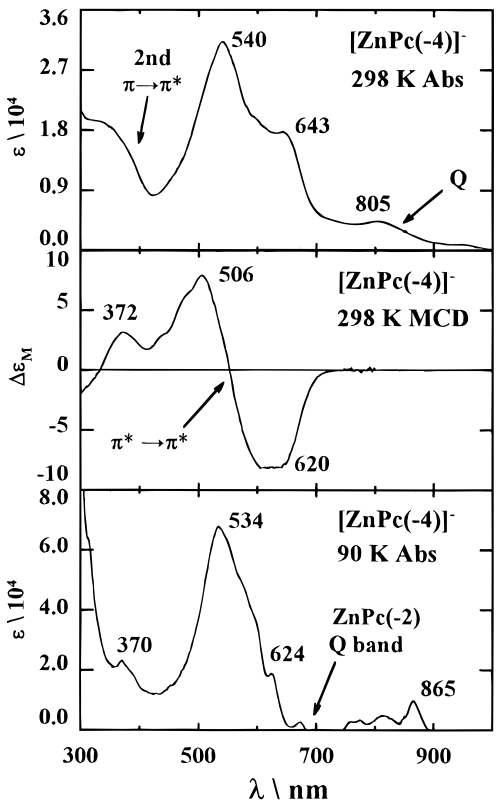

Figure 4. Room temperature absorption and MCD spectra of $[ZnPc(-4)]^{2-}$ recorded during the *in situ* spectroelectrochemical reduction of a 0.1 M TPAP solution of ZnPc in a DMF/piperidine (5:1) solvent mixture. The 90 K absorption spectra of $[ZnPc(-4)]^{2-}$ was recorded in DMF/hydrazine hydrate (5:2). There is a minor ZnPc(−2) impurity in the 90 K absorption spectrum.

Results

Absorption and MCD spectra of the three most important species of ZnPc are compared in Figure 3. Whereas the MCD spectra of the ring-oxidized species are dominated by derivative-shaped A terms, the MCD spectrum of the ring-reduced species is completely dominated by Gaussian-shaped B terms. The absorption and MCD spectra of the product of the two-electron ring-based reduction, $[ZnPc(-4)]^{2-}$, are shown in Figure 4. The absorption spectrum is dominated in the 450−700 nm region by an intense broad band at 540 nm (534 nm at 90 K) with a broad shoulder to lower energy at 643 nm (624 nm at 90 K). The MCD spectrum in this region is dominated by coupled sets of negative and positive B terms centered at 620 and 506 nm, respectively. The band centers of the major bands, therefore, appear to lie at significantly higher energy in the MCD spectrum. In the 700−1000 nm region, a weak absorption band centered at 805 nm (865 nm at 90 K) is virtually absent from the MCD spectrum. The 300−450 nm region contains a positive B term at 372 nm which is followed, to higher energy, by a negative B term below 300 nm. There is significant band sharpening in the 90 K absorption spectrum of $[ZnPc(-4)]^{2-}$ relative to that

(23) Ough, E. A.; Nyokong, T.; Creber, K. A. M.; Stillman, M. J. *Inorg. Chem.* **1988**, *27*, 2724.
(24) Ough, E. A.; Gasyna, Z.; Stillman, M. J. *Inorg. Chem.* **1991**, *30*, 2301.
(25) Mack, J.; Stillman, M. J. *J. Phys. Chem.* **1995**, *95*, 7935.
(26) Cory, M. G.; Hirose, H.; Zerner, M. C. *Inorg. Chem.* **1995**, *34*, 2969.
(27) CAChe Scientific, P.O. Box 500, Mail Station 13-400, Beaverton, OR 97077.
(28) Mack, J.; Kirkby, S.; Ough, E. A.; Stillman, M. J. *Inorg. Chem.* **1992**, *31*, 1717.
(29) Bobrovskii, A. P.; Kholmogorov, V. E. *J. Russ. Phys. Chem. (Engl. Transl.)* **1973**, *47*, 983.
(30) Gasyna, Z.; Browett, W. R.; Nyokong, T.; Kitchenham, R.; Stillman, M. J. *Chemom. Intell. Lab. Syst.* **1989**, *5*, 233.
(31) Mack, J.; Stillman, M. J. Unpublished program.
(32) Chen, G. C.; Yang, J. T. *Anal. Lett.* **1977**, *10*, 1195.
(33) Browett, W. R.; Stillman, M. J. *Comput. Chem.* **1987**, *11*, 73.

Table 1. Calculated Electronic Excitation Spectrum of $[ZnPc(-1)]^+$

no.[a]	sym[b]	calcd[c]	obsd[d]	wave function[e]	assignment[f]
1	$^2A_{1u}$				ground state
2, **3**	$^2E_{gx}$	10.4 (0.237)	12.1	$-0.961\|1e_g^* \leftarrow 1a_{1u}\rangle + 0.131\|1e_g^* \leftarrow 1a_{2u}\rangle^A + ...$	Q
11, **12**	$^2E_{gx}$	25.9 (0.109)	24.2	$-0.730\|1a_{1u} \leftarrow 2e_g\rangle + 0.295\|2e_g^* \leftarrow 1a_{1u}\rangle - 0.289\|1e_g^* \leftarrow 2b_{2u}\rangle^B + 0.204\|1e_g^* \leftarrow 1a_{2u}\rangle^B + ...$	$\pi \rightarrow \pi$
14, **18**	$^2E_{gx}$	28.4 (0.077)	25.8	$0.662\|2e_g^* \leftarrow 1a_{1u}\rangle - 0.288\|1a_{1u} \leftarrow 1e_g\rangle + 0.273\|2e_g^* \leftarrow 2b_{1u}\rangle^B - 0.248\|1a_{2u}^* \leftarrow 2e_g\rangle^B - 0.231\|1b_{1u}^* \leftarrow 2e_g\rangle^B + 0.228\|1a_{1u} \leftarrow 2e_g\rangle + ...$	second $\pi \rightarrow \pi^*$
19, **20**	$^2E_{gx}$	30.6 (0.237)	30.3	$-0.506\|1e_g^* \leftarrow 1a_{2u}\rangle^B - 0.439\|1e_g^* \leftarrow 1a_{2u}\rangle^A - 0.364\|1a_{1u} \leftarrow 3e_g\rangle + 0.279\|1e_g^* \leftarrow 1a_{2u}\rangle^B + 0.202\|2e_g^* \leftarrow 1a_{1u}\rangle + ...$	B1
26, **27**	$^2E_{gx}$	33.5 (0.085)	31.7	$-0.611\|1e_g^* \leftarrow 1b_{1u}\rangle^A - 0.320\|1e_g^* \leftarrow 1b_{1u}\rangle^B - 0.349\|1e_g^* \leftarrow 2a_{2u}\rangle^A - 0.206\|1e_g^* \leftarrow 2a_{2u}\rangle^B + ...$	B2
28, **31**	$^2E_{gx}$	34.7 (0.840)	36.1	$0.753\|3e_g^* \leftarrow 1a_{1u}\rangle - 0.347\|2e_g^* \leftarrow 1a_{1u}\rangle - 0.292\|1e_g^* \leftarrow 1a_{2u}\rangle^A + ...$	N
35	$^2A_{2g}$	36.1 (0.015)	19.6	$0.492\|1e_g^* \leftarrow e_u^N\rangle^A + 0.354\|1e_g^* \leftarrow e_u^N\rangle^B - 0.359\|1b_{2u}^* \leftarrow b_{1g}^N\rangle^A + 0.299\|1b_{2u}^* \leftarrow b_{1g}^N\rangle^B + ...$	$n \rightarrow \pi^*$

[a] The number of the state assigned in terms of ascending energy in the ZINDO calculation. Only states which result from allowed electronic transitions with a non-zero oscillator strength are included in the table. [b] The symmetry of the state under D_{4h} symmetry. [c] The calculated band energies (10^3 cm^{-1}), and oscillator strengths are given in parentheses. [d] Observed band energies (10^3 cm^{-1}) for $[MPc(-1)]^+$ (M = Mg, Zn) from the data of Nyokong *et al.*[18a] and Ough *et al.*[24] [e] The calculated wave functions based on the eigenvectors produced by the configuration interaction calculation of the ZINDO program.[44] [f] The assignment is described in the text. A and B refer to separate spin-allowed excited state configurations that are associated with one-electron transitions linking the same orbitals. N denotes orbitals associated with the aza-nitrogen lone pair orbitals.

of the 298 K spectrum, as has been seen previously in the cryogenic temperature absorption spectra of vitrified solutions of $ZnPc(-2)$[25] and $[ZnPc(-3)]^-$.[13]

At room temperature, irradiation of DMF/hydrazine hydrate solutions of $ZnPc(-2)$ through a Corning CS 2-73 filter, to ensure that light is absorbed only by the Q transition, results in reduction via the lowest energy triplet state to form $[ZnPc(-3)]^-$.[13] Irradiation with UV-light leads to significant side reactions that result in ring decomposition. Ferraudi has proposed that higher energy $n\pi^*$ states can be populated through irradiation in the UV-region.[34] These highly reactive states take part in hydrogen abstraction reactions that disrupt the π-system of the ring. No significant reduction is seen when vitrified solutions of $ZnPc(-2)$ are irradiated through a Corning CS 2-73 filter at cryogenic temperatures. The photoreduction mechanism via the T1 state of the (hydrazine)$ZnPc(-2)$ complex, which occurs at room temperature, will no longer be favored as the resulting radical pair can no longer dissociate in solution. However, prolonged irradiation with UV-light at cryogenic temperatures results in the formation of both $[ZnPc(-3)]^-$ and $[ZnPc(-4)]^{2-}$. As hydrazine absorbs significantly in the UV-region, competing photoreduction mechanisms that depend upon the photoexcitation of either the hydrazine or $ZnPc(-2)$ molecules result in the formation of both $[ZnPc(-3)]^-$ and $[ZnPc(-4)]^{2-}$.

While photochemical and electrochemical methods can be used to generate both $[MPc(-3)]^-$ and $[MPc(-4)]^{2-}$ species, chemical reduction methods have to be used to generate the more highly reduced $[MPc(-5)]^{3-}$ and $[MPc(-6)]^{4-}$ species.[3,11,35,36] Stable solutions of $[MPc(-5)]^{3-}$ and $[MPc(-6)]^{4-}$ have been prepared chemically by reaction *in vacuo* over sodium metal films in aprotic solvents such as DMF and tetrahydrofuran (THF).[3,11] Clack and Yandle[3] reported λ_{max} and relative band intensities for the $[MPc(-(2+n))]^{n-}$ ($n = 1-4$) species of a number of metal phthalocyanine complexes using this reduction method. The assignment of the species to the different spectra has been based largely upon EPR[37,38] and electrochemical evidence.[3,39,40] Room temperature MCD data have been reported for the $[MPc(-(2+n))]^{n-}$ ($n = 1-4$) species of MgPc by Linder *et al.*[11] using *in vacuo* sodium reduction in THF. It should be noted that the sign was inverted in the 300−500 nm portion of the $[MPc(-3)]^-$ spectrum and in the entire $[MPc(-4)]^{2-}$ spectrum. The data of Linder *et al.*,[11] as well as those of Clack and Yandle,[3] will be used to test the validity of the band assignment scheme that is proposed in this paper for reduced metal phthalocyanine species.

INDO Calculations. The ZnPc structure for our MO calculations was obtained through the use of a Tektronics, Inc., CAChe workstation.[27] The structure was refined using a modified MM2 force field calculation in the mechanics program of the CAChe system.[41] The structures of the $[ZnPc(-(2+n))]^{n-}$ ($n = -1-4$) species were optimized at the restricted Hartree−Fock self-consistent field (SCF) level,[42] in the case of the diamagnetic species, and at the restricted open-shell Hartree−Fock (ROHF) SCF level,[43] in the case of the paramagnetic species, using the ZINDO program in the CAChe software package.[44] These SCF optimizations were carried out at the intermediate neglect of differential overlap/1 (INDO/1)[45] level of approximation. The structures were then used to obtain calculated UV−vis absorption spectra using the spectroscopic INDO Hamiltonian (INDO/S),[43a,b] Tables 1−4, of the $[ZnPc(-(2+n))]^{n-}$ ($n = -1-2$) species and the energies of the frontier molecular orbitals of $[ZnPc(-5)]^{3-}$ and $[ZnPc(-6)]^{4-}$, Tables 5 and 6 (see Supporting Information). For the $[ZnPc(-(2+n))]^{n-}$ ($n = 0, 2, 4$) species, the active orbitals in the configuration interaction (CI) calculation were the 22 lowest

(34) Ferraudi, G. In *Phthalocyanine. Principles and Properties*; Leznoff, C. C., Lever A. B. P., Eds.; VCH Publications: New York, 1989; Vol. I, pp 291−340.
(35) Shablya, A. V.; Terenin, A. N. *Opt. Spectrosk.* **1960**, *9*, 533.
(36) Dodd, J. W.; Hush, N. S. *J. Chem. Soc.* **1964**, 4607.
(37) Guzy, C. M.; Raynor, J. B.; Stodulski, L. P.; Symons, M. C. R. *J. Chem. Soc. A* **1969**, *10*, 997.
(38) Clack, D. W.; Hush, N. S. *J. Am. Chem. Soc.* **1965**, *87*, 4238.
(39) Felton, R. H.; Linschitz, H. *Inorg. Chem.* **1966**, *88*, 1113.
(40) Clack, D. W.; Hush, N. S.; Woolsey, I. S. *Inorg. Chim. Acta* **1976**, *19*, 129.
(41) Purvis, G. D., III *Comput. Aided Mol. Des.* **1991**, *5*, 55.
(42) Roothaan, C. C. J. *Rev. Mod. Phys.* **1951**, *23*, 69.
(43) (a) McWeeny, R.; Diercksen, G. J. *Chem. Phys.* **1968**, *49*, 4852. (b) Guest, M. F.; Saunders, V. R. *Mol. Phys.* **1968**, *28*, 819. (c) Binkley, J. S.; Pople, J. A.; Dobosh, P. A. *Mol. Phys.* **1974**, *28*, 1423. (d) Davidson, E. R. *Chem. Phys. Lett.* **1973**, *21*, 565. (e) Faegri, K.; Manne, R. *Mol. Phys.* **1976**, *31*, 1037. (f) Hsu, H.; Davidson, E. R.; Pitzer, R. M. *J. Chem. Phys.* **1976**, *65*, 609.
(44) (a) Ridley, J. E.; Zerner, M. C. *Theor. Chim. Acta* **1973**, *32*, 111. (b) Zerner, M. C.; Loew, G. H.; Kirchner, R. F.; Mueller-Westerhoff, U. T. *J. Am. Chem. Soc.* **1980**, *102*, 589. (c) Ridley, J. E.; Zerner, M. C. *Theor. Chim. Acta* **1976**, *42*, 223. (d) Bacon, A.; Zerner, M. C. *Theor. Chim. Acta* **1979**, *53*, 21. (e) Head, J.; Zerner, M. C. *Chem. Phys. Lett.* **1985**, *122*, 264. (f) Head, J.; Zerner, M. C. *Chem. Phys. Lett.* **1986**, *131*, 359. (g) Anderson, W.; Edwards, W. D.; Zerner, M. C. *Inorg. Chem.* **1986**, *25*, 2728. (h) Edwards, W. D.; Zerner, M. C. *Theor. Chim. Acta* **1987**, *72*, 347. (i) Kotzian, M.; Roesch, N.; Zerner, M. C. *Theor. Chim. Acta* **1992**, *81*, 201. (j) Kotzian, M.; Roesch, N.; Zerner, M. C. *Int. J. Quantum Chem.* **1991**, 545.
(45) Pople, J. A.; Beveridge, D.; Dobash, P. A. *Chem. Phys.* **1967**, *47*, 2026.

Table 2. Calculated Electronic Excitation Spectrum of ZnPc(−2)

no.[a]	sym[b]	calcd[c]	obsd[d]	wave function[e]	assignment[f]
1	$^1A_{1g}$				ground state
2, **3**	$^1E_{ux}$	14.8 (0.903)	14.8	$-0.950\|1e_g^* \leftarrow 1a_{1u}\rangle + 0.260\|1e_g^* \leftarrow 1a_{2u}\rangle + ...$	Q
6, **7**	$^1E_{ux}$	30.0 (0.023)		$-0.978\|2e_g^* \leftarrow 1a_{1u}\rangle - 0.073\|4e_g^* \leftarrow 1a_{1u}\rangle + ...$	second $\pi \rightarrow \pi^*$
13	$^1A_{2u}$	34.1 (0.032)	16.5	$0.561\|1e_g^* \leftarrow e_u^N\rangle - 0.472\|1b_{2u}^* \leftarrow b_{1g}^N\rangle + ...$	$n \rightarrow \pi^*$
14, **15**	$^1E_{ux}$	34.3 (0.428)	25.5	$0.808\|1e_g^* \leftarrow 1b_{1u}\rangle - 0.255\|1b_{2u}^* \leftarrow 1e_g\rangle - 0.221\|1e_g^* \leftarrow 1a_{2u}\rangle + ...$	B1
16, **17**	$^1E_{ux}$	34.7 (2.233)	29.9	$-0.815\|1e_g^* \leftarrow 1a_{2u}\rangle - 0.348\|3e_g^* \leftarrow 1a_{1u}\rangle - 0.252\|1e_g^* \leftarrow 1b_{1u}\rangle + 0.228\|1e_g^* \leftarrow 1a_{1u}\rangle + ...$	B2
21, **22**	$^1E_{ux}$	36.5 (0.330)	33.6	$-0.574\|3e_g^* \leftarrow 1a_{1u}\rangle + 0.371\|1e_g^* \leftarrow 1a_{2u}\rangle - 0.259\|1b_{1u}^* \leftarrow 1e_g\rangle - 0.251\|2e_g^* \leftarrow 1b_{2u}\rangle - 0.222\|2e_g^* \leftarrow 1b_{1u}\rangle + ...$	N
29, **31**	$^1E_{ux}$	39.0 (0.014)	36.2	$-0.635\|3e_g^* \leftarrow 1a_{1u}\rangle - 0.593\|1e_g^* \leftarrow 2b_{2u}\rangle + 0.278\|1e_g^* \leftarrow 2a_{1u}\rangle + 0.216\|1b_{2u} \leftarrow 2e_g^*\rangle + ...$	L
34, **35**	$^1E_{ux}$	41.1 (0.019)	40.7	$-0.744\|1e_g^* \leftarrow 2a_{2u}\rangle - 0.451\|1e_g^* \leftarrow 1b_{1u}\rangle - 0.293\|1e_g^* \leftarrow 1b_{2u}\rangle + 0.255\|3e_g^* \leftarrow 1a_{1u}\rangle + ...$	C

[a] The number of the state assigned in terms of ascending energy in the ZINDO calculation. Only states which result from allowed electronic transitions with a non-zero oscillator strength are included in the table. [b] The symmetry of the state under D_{4h} symmetry. [c] The calculated band energies (10^3 cm^{-1}), and oscillator strengths are given in parentheses. [d] Observed energies (10^3 cm^{-1}) from the data of Nyokong *et al.*[22] [e] The calculated wave functions based on the eigenvectors produced by the configuration interaction calculation of the ZINDO program.[44] [f] The assignment is described in the text. N denotes orbitals that are associated with the aza-nitrogen lone pair orbitals.

energy unoccupied and 22 highest energy occupied molecular orbitals. For the $[ZnPc(-(2 + n))]^{n-}$ ($n = 1, 3, 5$) species, the active orbitals in the CI calculation were the 15 lowest energy unoccupied and 15 highest energy occupied molecular orbitals. The existing band nomenclature which has been developed for assigning the spectral bands of the MPc(−2) species over the last decade[18,22−25] is retained in this present paper. However, the association of specific one-electron transitions with each band has been modified based upon the results of the ZINDO calculation. Further, minor changes to the band and transition nomenclature of the radical cation and radical anion species have been made on this basis.

Spectral Band Assignments. The MPc(−2) Species. The absorption spectra of ZnPc(−2) includes, Figure 3, an intense Q band (ϵ ca. 10^5) near 670 nm, followed by a series of vibrational components, Q_{vib}. The ground states of divalent, main group D_{4h} MPc(−2) complexes are $^1A_{1g}$, while the accessible $\pi \rightarrow \pi^*$ excited states will be degenerate, ^1E_u (*x*/*y*-polarized), Figure 5. Our ZINDO calculation for the electronic spectrum of ZnPc(−2) species, Table 1, is very similar to that of the calculation by Cory *et al.* of MgPc(−2).[26] The splitting of the $1a_{1u}$ and $1a_{2u}$ HOMOs of MPc(−2) is so great that the $1a_{1u} \rightarrow 2e_g^*$ transition is predicted to lie at lower energy than the $1a_{2u} \rightarrow 1e_g^*$ transition, Figure 5. A very weak, derivative-shaped signal seen in an MCD spectrum reported previously for MgPc(−2)[18b,23] at around 435 nm may be an A term associated with this transition. This second $\pi \rightarrow \pi^*$ transition is not predicted to have significant intensity, however, as there is almost no mixing with the allowed B1 transition. The higher energy excited states are found to mix to such an extent that the traditional one-electron transition descriptions are not particularly meaningful. The B1 and B2 bands seen in the spectrum of (CN)ZnPc(−2)[18a,b] at 386 and 331 nm arise primarily from the $1a_{2u} \rightarrow 1e_g^*$ and $1b_{1u} \rightarrow 1e_g^*$ transitions, as expected, Figure 5. The N and L bands at 298 and 276 nm are found to have significant contributions from the $1a_{1u} \rightarrow 3e_g^*$ transition of the π-system, Table 2, and the C band at 246 nm is found to arise primarily from the $2a_{2u} \rightarrow 1e_g^*$ transition. Low-temperature MCD and Shpol'skii matrix emission studies have indicated that there is a *z*-polarized transition at 604 nm, just to the blue of the Q transition of MPc(−2) complexes.[25,46,47] The band is believed to arise from an $n \rightarrow \pi^*$ transition out of the aza-nitrogen lone pair orbitals. An $n \rightarrow \pi^*$ band is predicted at 293 nm by the ZINDO calculation, well to the blue of the experimentally observed band.

The $[MPc(-1)]^+$ Species. The band assignment of $[MPc(-1)]^+$ (M = Mg, Zn) is more complicated than that of MPc(−2) as there is an additional A term to the red of the B1/B2 region at 413 nm and an intense B term at 509 nm arising from a transition to a nondegenerate excited state,[18,24,48] Figure 3. Both of these transitions have previously been assigned as $\pi \rightarrow \pi$ transitions into the partially filled LUMO.[48] Recently, the 509 nm transition was reassigned as an $n \rightarrow \pi^*$ transition linking the lone pair orbitals of the aza-nitrogens and the LUMO of the π-system on the basis of a detailed band deconvolution analysis of the absorption and MCD spectra of ZnPc(−2) recorded at cryogenic temperatures that identified an $n \rightarrow \pi^*$ transition slightly to the blue of the Q transition.[25] As the 509 nm transition gives rise to an intense *z*-polarized Faraday B term rather than an *x*/*y*-polarized A term, the excited state is clearly nondegenerate. No spectral band with significant *z*-polarized intensity is predicted in the 300−1000 nm region by the ZINDO calculations, Tables 1 and 2, for either ZnPc(−2) or $[ZnPc(-1)]^+$. The ZINDO calculation of $[ZnPc(-1)]^+$ predicts that the lowest energy *z*-polarized band should lie at 277 nm. This strongly suggests that the ZINDO calculation does not provide a good estimate of the energies of the nonbonding aza-nitrogen lone pair orbitals. The additional A term at 413 nm was assigned to the lowest energy $\pi \rightarrow \pi$ transition into the partially filled HOMO, Figure 6.[25] The ZINDO calculation predicts that bands identified at 387, 330, and 315 nm through spectral deconvolution[24] of the absorption and MCD spectra of $[MgPc(-1)]^+$ arise primarily from the second $\pi \rightarrow \pi^*$, the B1, and the B2 transitions, respectively. As the second $\pi \rightarrow \pi^*$ transition mixes much more significantly with the other higher energy $\pi \rightarrow \pi^*$ transitions than is the case in the ZnPc(−2) spectrum, three intense A terms are seen in the B1/B2 region. The major contribution to the band at 275 nm appears to be the $1a_{1u} \rightarrow 3e_g^*$ transition that gives rise to the N band of MPc(−2), Table 1.

The $[MPc(-3)]^-$ Species. The cryogenic-temperature MCD spectrum of the one-electron ring-reduced species is completely dominated by B terms, rather than the anticipated C terms.[13,21] Analysis indicates that there is a substantial static Jahn−Teller splitting of the ground state as the MCD spectra of [MgPc(−

(46) (a) Huang, T. H.; Reickhoff, K. E.; Voight, E. M. *J. Chem. Phys.* **1982**, *77*, 3424. (b) Huang, T. H.; Reickhoff, K. E.; Voight, E. M. *J. Phys. Chem.* **1981**, *85*, 3322.

(47) VanCott, T. C.; Rose, J. L; Misener, G. C.; Williamson, B. E.; Schrimpf, A. E.; Boyle, M. E.; Schatz, P. N. *J. Phys. Chem.* **1989**, *93*, 2999.

(48) Ough, E. A. Ph.D. Thesis, University of Western Ontario, 1993.

Table 3. Calculated Electronic Excitation Spectrum of $[ZnPc(-3)]^-$

no.[a]	sym[b]	calcd[c]	obsd[d]	wave function[e]	assignment[f]
1	$^2A_2$				ground state
3	$^2A_2$	8.87 (0.097)	10.4	$0.842\|1a_2^* \leftarrow 1a_2\rangle + 0.370\|2a_2^* \leftarrow 2a_2\rangle - 0.281\|2a_2^* \leftarrow 1a_2\rangle^B + ...$	Q_z
4	$^2B_2$	10.4 (0.069)	10.8	$-0.683\|1b_2^* \leftarrow 1a_2\rangle^B + 0.438\|1b_2^* \leftarrow 1a_2\rangle^A - 0.435\|2b_2^* \leftarrow 2a_2^*\rangle + 0.138\|4b_2^* \leftarrow 1a_2\rangle^B + ...$	Q_x
5	$^2A_2$	16.6 (0.594)	15.7	$0.797\|2a_2^* \leftarrow 1a_2^*\rangle - 0.356\|1a_2^* \leftarrow 1a_2\rangle + 0.238\|1b_2^* \leftarrow 1b_2\rangle + 0.156\|3a_2^* \leftarrow 1a_2\rangle^B - 0.146\|4a_2^* \leftarrow 1a_2^*\rangle + ...$	$\pi^* \rightarrow \pi^*_z$
6	$^2B_2$	17.0 (0.292)	17.5	$-0.665\|3b_2^* \leftarrow 1a_2^*\rangle - 0.423\|2b_2^* \leftarrow 1a_2^*\rangle - 0.380\|1b_2^* \leftarrow 1a_2\rangle^A + 0.148\|1b_2^* \leftarrow 1a_2\rangle^B - 0.195\|3b_2^* \leftarrow 1a_2\rangle^B - 0.150\|2b_2^* \leftarrow 1a_2\rangle^B + ...$	$\pi^* \rightarrow \pi^*_x$
7	$^2B_2$	18.9 (0.469)	11.4	$-0.508\|1b_2^* \leftarrow 1a_2\rangle^A + 0.434\|4b_2^* \leftarrow 1a_2\rangle^B - 0.448\|4b_2^* \leftarrow 1a_2^*\rangle + 0.257\|3b_2^* \leftarrow 1a_2^*\rangle - 0.235\|2b_2^* \leftarrow 1a_2^*\rangle + 0.209\|2b_2^* \leftarrow 1a_2\rangle^B + ...$	Q_x/second $\pi^* \rightarrow \pi^*_x$
8	$^2B_2$	21.5 (0.207)		$-0.419\|1b_2^* \leftarrow 1a_2\rangle^A - 0.325\|1b_2^* \leftarrow 1a_2\rangle^B - 0.420\|4b_2^* \leftarrow 1a_2\rangle^B - 0.420\|4b_2^* \leftarrow 1a_2^*\rangle + 0.298\|3b_2^* \leftarrow 1a_2^*\rangle - 0.226\|6b_2^* \leftarrow 1a_2^*\rangle + ...$	Q_x/second $\pi^* \rightarrow \pi^*_x$
12	$^2B_2$	25.5 (0.012)		$0.668\|2b_2^* \leftarrow 1a_2\rangle^A - 0.456\|2b_2^* \leftarrow 1a_2\rangle^B - 0.221\|3b_2^* \leftarrow 1a_2\rangle^A + 0.266\|3b_2^* \leftarrow 1a_2\rangle^B + ...$	
13	$^2A_2$	25.6 (0.130)		$-0.564\|4a_2^* \leftarrow 1a_2^*\rangle - 0.512\|4a_2^* \leftarrow 1a_2\rangle^A - 0.361\|3a_2^* \leftarrow 1a_2^*\rangle - 0.200\|6a_2^* \leftarrow 1a_2^*\rangle + ...$	second $\pi^* \rightarrow \pi^*_z$
14	$^2B_2$	26.0 (0.179)	23.0	$-0.631\|1a_2^* \leftarrow 3b_2\rangle + 0.380\|1a_2^* \leftarrow 2b_2\rangle + 0.366\|1a_2^* \leftarrow 1b_2\rangle + ...$	$B1/B2_x$
17	$^2B_2$	27.3 (0.124)	24.8	$0.631\|4b_2^* \leftarrow 1a_2\rangle^A - 0.216\|4b_2^* \leftarrow 1a_2\rangle^B + 0.314\|1a_2^* \leftarrow 1b_2\rangle + 0.305\|4b_2^* \leftarrow 1a_2^*\rangle - 0.252\|1a_2^* \leftarrow 2b_2\rangle - 0.212\|1a_2^* \leftarrow 1b_2\rangle + ...$	second $\pi \rightarrow \pi^*_x$
18	$^2A_2$	27.6 (0.061)		$-0.429\|3a_2^* \leftarrow 1a_2\rangle^A + 0.305\|3a_2^* \leftarrow 1a_2\rangle^B + 0.351\|5a_2^* \leftarrow 1a_2\rangle^B - 0.234\|6a_2^* \leftarrow 1a_2\rangle^B + ...$	
19	$^2B_2$	28.3 (0.173)		$0.528\|4b_2^* \leftarrow 1a_2\rangle^A - 0.204\|4b_2^* \leftarrow 1a_2\rangle^B - 0.438\|1a_2^* \leftarrow 1b_2\rangle + 0.249\|2a_2^* \leftarrow 1b_2\rangle + 0.240\|1a_2^* \leftarrow 2b_2\rangle + ...$	second $\pi \rightarrow \pi^*_x$
23	$^2B_2$	30.8 (0.486)		$-0.400\|3b_2^* \leftarrow 1a_2\rangle^A + 0.258\|3b_2^* \leftarrow 1a_2\rangle^B - 0.304\|2a_2^* \leftarrow 1a_2\rangle^A + 0.327\|1a_2^* \leftarrow 3b_2\rangle + 0.305\|1a_2^* \leftarrow 2b_2\rangle - 0.292\|1a_2^* \leftarrow 5b_2\rangle + 0.219\|1a_2^* \leftarrow 1b_2\rangle + ...$	$B1/B2_x$
24	$^2A_2$	31.2 (0.031)		$0.539\|2a_2^* \leftarrow 1a_2\rangle^B - 0.303\|5a_2^* \leftarrow 1a_2^*\rangle^B + 0.243\|1a_2^* \leftarrow 2a_2\rangle + 0.232\|3a_2^* \leftarrow 1a_2\rangle^A - 0.212\|5a_2^* \leftarrow 1a_2\rangle^B - 0.206\|4a_2^* \leftarrow 1a_2\rangle^B + ...$	
25	$^2B_2$	31.9 (0.255)		$0.686\|3b_2^* \leftarrow 1a_2\rangle^A + 0.262\|1a_2^* \leftarrow 1b_2\rangle - 0.205\|6b_2^* \leftarrow 1a_2^*\rangle - 0.202\|5b_2^* \leftarrow 1a_2^*\rangle^B + ...$	$B1/B2_x$
26	$^2A_2$	32.0 (0.032)		$0.397\|1b_2^* \leftarrow 2b_2\rangle^B - 0.303\|2a_2^* \leftarrow 1a_2\rangle^B - 0.326\|2a_2^* \leftarrow 1a_2^*\rangle - 0.282\|4a_2^* \leftarrow 1a_2^*\rangle + 0.235\|3a_2^* \leftarrow 1a_2^*\rangle + 0.216\|5a_2^* \leftarrow 1b_2\rangle + 0.217\|3a_2^* \leftarrow 1a_2\rangle^A + 0.215\|1b_2^* \leftarrow 4b_2\rangle^B + 0.202\|1b_2^* \leftarrow 1b_2\rangle^B + ...$	
27	$^2B_2$	32.6 (0.141)		$0.293\|2b_2^* \leftarrow 1a_2\rangle^B + 0.175\|5b_2^* \leftarrow 1a_2\rangle^A + 0.245\|1a_2^* \leftarrow 1b_2\rangle - 0.263\|3b_2^* \leftarrow 1a_2\rangle + 0.255\|6b_2^* \leftarrow 1a_2\rangle - 0.259\|3a_2^* \leftarrow 4b_2\rangle^B - 0.223\|1b_2^* \leftarrow 3a_2\rangle^B + ...$	
28	$^2A_2$	32.7 (0.045)		$0.519\|1a_2^* \leftarrow 2a_2\rangle - 0.249\|6a_2^* \leftarrow 1a_2\rangle - 0.230\|3a_2^* \leftarrow 1a_2^*\rangle^A + 0.206\|4a_2^* \leftarrow 1a_2\rangle + 0.203\|1b_2^* \leftarrow 2b_2\rangle^B + ...$	
30	$^2A_2$	33.7 (0.023)		$0.408\|1b_2^* \leftarrow 2b_2\rangle^B - 0.336\|4b_2^* \leftarrow 2b_2\rangle^B - 0.252\|3a_2^* \leftarrow 2b_2\rangle^A + 0.207\|3a_2^* \leftarrow 1a_2\rangle^B + 0.225\|2a_2^* \leftarrow 1a_2\rangle^B + 0.210\|4b_2^* \leftarrow 1b_2\rangle^B + ...$	
31	$^2A_2$	34.0 (0.274)		$-0.578\|1b_2^* \leftarrow 1b_2\rangle^B + 0.187\|1b_2^* \leftarrow 2b_2\rangle^A - 0.265\|4b_2^* \leftarrow 2b_2\rangle^B + 0.222\|3a_2^* \leftarrow 1a_2\rangle^A - 0.219\|3a_2^* \leftarrow 1a_2\rangle^B - 0.222\|5a_2^* \leftarrow 1a_2\rangle^A + ...$	$B1/B2_z$
33	$^2B_1$	34.5 (0.013)		$-0.698\|1a_2^* \leftarrow 2b_1^N\rangle - 0.430\|1b_2^* \leftarrow 2a_1^N\rangle - 0.181\|1a_2^* \leftarrow 1b_1^N\rangle - 0.136\|6a_2^* \leftarrow 1b_1^N\rangle + ...$	$n \rightarrow \pi^*$
34	$^2A_2$	34.8 (0.115)		$0.370\|1a_2^* \leftarrow 3a_2\rangle + 0.338\|5a_2^* \leftarrow 1a_2\rangle^A - 0.132\|5a_2^* \leftarrow 1a_2\rangle^B + 0.272\|1b_2^* \leftarrow 1b_2\rangle^A - 0.171\|1b_2^* \leftarrow 1b_2\rangle^B - 0.282\|2a_2^* \leftarrow 1a_2\rangle^A + ...$	
36	$^2A_2$	35.1 (0.352)		$-0.473\|5a_2^* \leftarrow 1a_2\rangle^A + 0.227\|1b_2^* \leftarrow 1b_2\rangle^A + 0.291\|1b_2^* \leftarrow 2b_2\rangle^A - 0.159\|1b_2^* \leftarrow 2b_2\rangle^B + ...$	

[a] The number of the state assigned in terms of ascending energy in the ZINDO calculation. Only states which result from allowed electronic transitions with a calculated oscillator strength greater than 0.01 are included in the table. [b] The symmetry of the state under C_{2v}(III) symmetry. [c] The calculated band energies (10^3 cm^{-1}), and oscillator strengths are given in parentheses. [d] Observed band energies (10^3 cm^{-1}) from the data of Mack and Stillman.[13] [e] The calculated wave functions based on the eigenvectors produced by the configuration interaction calculation of the ZINDO program.[44] [f] The assignment is described in the text. A and B refer to separate spin-allowed excited state configurations associated with one-electron transitions linking the same orbitals. N denotes orbitals that are associated with the aza-nitrogen lone pair orbitals.

3)]$^-$ and $[ZnPc(-3)]^-$ show no temperature dependence due to near degeneracy in the ground state. The MCD data were analyzed, Figure 3, to suggest that the separation of the coupled *x*- and *y*-polarized bands was due to a loss in planarity in the nonaromatic anion radical ring. The recent MO study by Cory *et al.*[26] suggested that ring planarity is retained and that the species has D_{2h} symmetry. In the absence of definitive X-ray crystallographic data, C_{2v} symmetry has been assumed for $[ZnPc(-3)]^-$ in Figures 7 and 8, as the molecular orbitals obtained in our ZINDO calculation for $[ZnPc(-3)]^-$ have C_{2v}-(III) rather than D_{2h} symmetry properties.[49] Under C_{2v}(III) symmetry, the Q, B1, and B2 transitions of ZnPc(−2) and the new $\pi^* \rightarrow \pi^*$ transition are allowed for $[ZnPc(-3)]^-$ with *x* - and *z*-polarized bands significantly separated in energy, Figure 7. The *z*-axis of $[ZnPc(-3)]^-$ under C_{2v}(III) symmetry corresponds to the *y*-axis of ZnPc(−2) under D_{4h} symmetry. A further effect of C_{2v}(III) symmetry is to allow $\pi \rightarrow \pi^*$, $\pi^* \rightarrow \pi^*$, and $n \rightarrow \pi^*$ transitions which would be parity forbidden under D_{4h} symmetry, Table 3. The poorer orbital overlap of the ground and excited states of these transitions will, however, significantly reduce the intensity of the associated spectral bands relative to that of the bands that arise from the parity allowed $\pi^* \rightarrow \pi^*$ and $\pi \rightarrow \pi^*$ transitions.

The Q, second $\pi \rightarrow \pi^*$, and B1 transitions of the neutral MPc(−2) species, and the new $\pi^* \rightarrow \pi^*$ transitions are, therefore, expected to be primarily responsible for the three distinct sets of coupled, oppositely-signed B terms that are observed in the MCD spectrum of $[ZnPc(-3)]^-$ at 958/925, 635/569, and 434/383 nm.[13] Michl has developed a detailed theory

(49) Mack, J.; Stillman, M. J. Manuscript in preparation.

Table 4. Calculated Electronic Excitation Spectrum of $[ZnPc(-4)]^{2-}$

no.[a]	sym[b]	calcd[c]	obsd[d]	wave function[e]	assignment[f]
1	^1A_g				ground state
3	$^1B_{2u}$	17.9 (1.025)	16.1	$-0.983\|1a_u^* \leftarrow 1b_{2g}^*\rangle + ...$	$\pi^* \rightarrow \pi^*_y$
4	$^1B_{3u}$	18.9 (0.153)	19.7	$0.890\|1b_{1u}^* \leftarrow 1b_{2g}^*\rangle - 0.294\|2b_{1u}^* \leftarrow 1b_{2g}^*\rangle + ...$	$\pi^* \rightarrow \pi^*_x$
6	$^1B_{3u}$	20.8 (1.347)	11.6	$0.903\|1b_{3g}^* \leftarrow 1a_u\rangle + 0.331\|2b_{1u}^* \leftarrow 1b_{2g}^*\rangle + 0.163\|2b_{3g}^* \leftarrow 1a_u\rangle - 0.122\|1b_{1u}^* \leftarrow 1b_2^*\rangle + ...$	Q_x
8	$^1B_{3u}$	21.4 (0.174)		$0.785\|2b_{1u}^* \leftarrow 1b_{2g}^*\rangle + 0.408\|1b_{1u}^* \leftarrow 1b_{2g}^*\rangle + 0.298\|1b_{3g}^* \leftarrow 1a_u\rangle + 0.264\|2b_{3g}^* \leftarrow 1a_u\rangle + ...$	second $\pi^* \rightarrow \pi^*_x$
11	$^1B_{2u}$	28.1 (0.435)		$0.792\|2a_u^* \leftarrow 1b_{2g}^*\rangle + 0.517\|2b_{2g}^* \leftarrow 1a_u\rangle + 0.203\|3b_{2g}^* \leftarrow 1a_u\rangle + ...$	second $\pi^* \rightarrow \pi^*_y$
13	$^1B_{2u}$	29.5 (0.095)		$0.831\|2b_{2g}^* \leftarrow 1a_u\rangle - 0.488\|2a_u^* \leftarrow 1b_{2g}^*\rangle + ...$	second $\pi \rightarrow \pi^*_y$
15	$^1B_{3u}$	33.1 (0.274)		$-0.730\|3b_{1u}^* \leftarrow 1b_{2g}^*\rangle - 0.566\|2b_{3g}^* \leftarrow 1a_u\rangle + 0.308\|2b_{1u}^* \leftarrow 1b_{2g}^*\rangle + ...$	third $\pi^* \rightarrow \pi^*_x$
17	$^1B_{2u}$	34.3 (0.093)		$-0.777\|3a_u^* \leftarrow 1b_{2g}^*\rangle - 0.332\|1b_{3g}^* \leftarrow 2b_{1u}\rangle - 0.328\|3b_{2g}^* \leftarrow 1a_u\rangle + ...$	third $\pi^* \rightarrow \pi^*_y$
18	$^1B_{1u}$	34.7 (0.024)		$0.699\|1b_{2g}^* \leftarrow 1b_{3u}^N\rangle + 0.544\|1a_u^* \leftarrow 1b_{1g}^N\rangle + ...$	$n \rightarrow \pi^*$
19	$^1B_{2u}$	35.0 (1.267)		$-0.855\|1b_{3g}^* \leftarrow 1b_{1u}\rangle - 0.226\|1a_u^* \leftarrow 1b_{2g}\rangle + ...$	$B1_y$
21	$^1B_{3u}$	35.5 (0.079)		$-0.698\|2b_{3g}^* \leftarrow 1a_u\rangle + 0.581\|3b_{1u}^* \leftarrow 1b_{2g}^*\rangle + 0.249\|3b_{3g}^* \leftarrow 1a_u\rangle + ...$	second $\pi \rightarrow \pi^*_x$

[a] The number of the state assigned in terms of ascending energy by the ZINDO calculation. Only states which result from allowed electronic transitions with a non-zero oscillator strength are included in the table. [b] The symmetry of the state under D_{2h}(II) symmetry. [c] The calculated band energies (10^3 cm^{-1}), and oscillator strengths are given in parentheses. [d] Observed band energies from the data reported in this paper. [e] The calculated wave functions based on the eigenvectors produced by the configuration interaction calculation of the ZINDO program.[44] [f] The assignment is described in the text. N denotes orbitals that are associated with the aza-nitrogen lone pair orbitals.

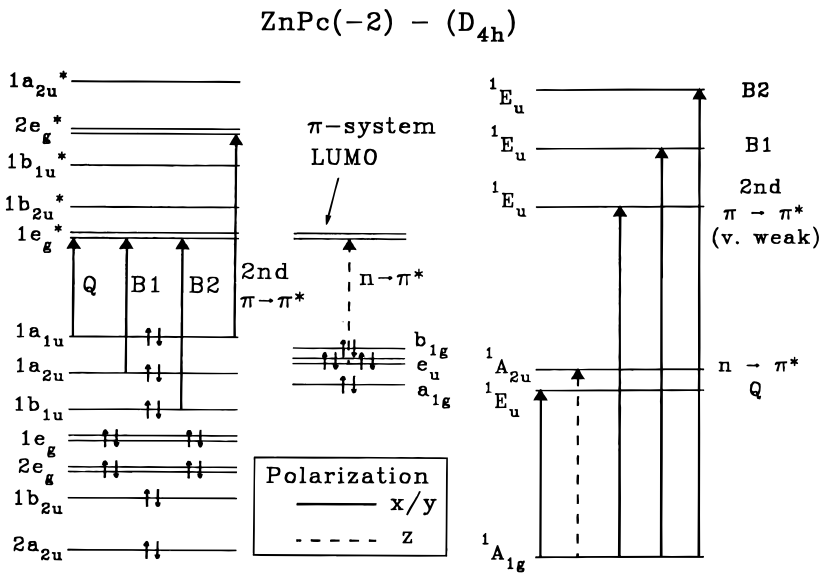

Figure 5. Molecular orbital and state level diagrams of ZnPc(−2) showing the transitions that are predicted to give rise to absorption bands in the 300−1000 nm range. The Q, B1, and B2 bands have been identified through spectral deconvolution studies[18,24] on the basis of Gouterman's SCMO-PPP-CI model.[17] Our ZINDO calculation, Table 2, of the absorption spectrum of ZnPc(−2) predicts the presence of a much weaker second $\pi \rightarrow \pi^*$ transition. The $n \rightarrow \pi^*$ transition is placed between the Q and B1 transitions on the basis of a spectral deconvolution analysis of the absorption and MCD spectra of (CN)ZnPc(−2)[25] recorded at cryogenic temperatures. The orbital ordering on the left is based on the results of our ZINDO calculation, Table 2.

to predict the signs of pairs of oppositely-signed B terms that arise from separate *x*- and *y*-polarized transitions into the degenerate π-orbitals of cyclic polyene molecules in which the degeneracy has been broken by a perturbation to the molecular geometry.[50] The equivalent intensities of the 635/569 nm pair of B terms is consistent with field-induced mixing between two major transitions to a pair of close lying empty orbitals, as the intensity mechanism of Faraday B terms depends upon the field-induced mixing of close lying states. These bands were, therefore, assigned to the $\pi^* \rightarrow \pi^*$ transition, Figure 7. The pair of bands centered at 958 and 925 nm exhibit an inequivalence in the B term intensities, which indicates that the transitions involve an electron going into a partially filled orbital. These bands can, therefore, be assigned to the Q transition. The −/+ order in the signs of the coupled Faraday B terms to high energy is consistent with a set of transitions in which the orbital angular momentum of the excited states is greater than that in the ground state.[50]

Our ZINDO calculation for $[ZnPc(-3)]^-$, Table 3, predicts that there should be three bands associated primarily with the Q transition at 1127, 963, and 529 nm. The far smaller energy splittings observed between the three intense coupled B terms in the 850−1000 nm region[25,28] indicate that the ZINDO calculation of the absorption spectrum of both $[MgPc(-3)]^-$ [26] and $[ZnPc(-3)]^-$, Table 3, significantly overestimate the splitting of the bands associated with the Q transition. The recent MO calculation by Cory et al.[26] on $[MgPc(-3)]^-$ suggested that four major electronic transitions give rise to the observed bands in the 500−800 nm region. These authors assigned four major absorption maxima and shoulders in the absorption spectrum at 643, 590, 569, and 530 nm to bands arising from transitions to A_u, B_{1u}, B_{1u}, and A_u excited states, respectively. These transitions would be predicted to give rise to two sets of coupled, oppositely-signed *x*- and *z*-polarized B

(50) (a) Michl, J. *J. Am. Chem. Soc.* **1978**, *100*, 6801. (b) Michl, J. *Pure Appl. Chem.* **1980**, *52*, 1549.
(51) (a) Piepho, S. B.; Schatz, P. N. In *Group Theory in Spectroscopy with Applications to Magnetic Circular Dichroism*; Wiley: New York, 1983. (b) Stephens, P. J. *Adv. Chem. Phys.* **1976**, *35*, 197.

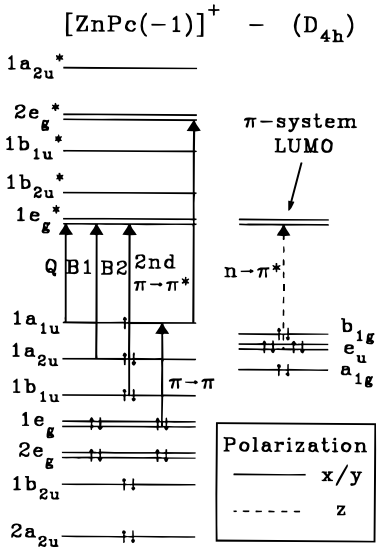

Figure 6. Molecular orbital diagram for the inner cyclic polyene ring and aza-nitrogen lone pair orbitals of $[ZnPc(-1)]^+$, assuming D_{4h} symmetry. The orbital ordering on the left is based on the results of our ZINDO calculation, Table 1.

terms in the MCD spectrum. This is not consistent with our MCD spectral data, Figure 3, which is clearly dominated by a single pair of oppositely-signed B terms at 643 and 569 nm. Our ZINDO calculation of the absorption spectrum of $[ZnPc(-3)]^-$, Table 3, predicts the presence of three major bands at 600, 587, and 529 nm, Table 3. As the 529 nm band predicted by our ZINDO calculation is associated primarily with the Q transition, it can be ignored. The calculation for $[ZnPc(-3)]^-$, therefore, suggests that only two bands, at 600 and 588 nm, give rise to significant intensity in the 500−800 nm region. These bands are associated primarily with the $\pi^* \rightarrow \pi^*$ transition that we have assigned to the bands observed at 635 and 569 nm. The complexity seen in the absorption spectrum in this region may be due to the coincident presence of $n \rightarrow \pi^*$ transitions, such as those seen in the spectra of $ZnPc(-2)$ and $[ZnPc(-1)]^+$.[25] The spectral deconvolution analysis of the optical spectra of $[ZnPc(-3)]^-$ [13] indicated that there are two major overlapping sets of B terms in the 300−450 nm region. The ZINDO calculation, Table 3, suggests that the second $\pi \rightarrow \pi^*$, B1, and B2 transitions contribute significantly to the numerous bands in this region, Table 3. The predicted degree of mixing between the excited states is so great, however, that the assignment of individual bands to specific one-electron transitions would not be particularly meaningful in this region of the spectrum, Table 3.

The $[MPc(-4)]^{2-}$ Species. Previous workers have reported that there is no EPR signal[37,40] for this species. We can, therefore, conclude that the two electrons are paired in the lower energy orbital of the Jahn−Teller split LUMO, Figure 7. Our ZINDO calculation suggests that the $[ZnPc(-4)]^{2-}$ species has D_{2h}(II) symmetry[49] which results in a complete lifting of the ground and excited state orbital degeneracies similar to that seen in the $[ZnPc(-3)]^-$ species. As the orbital symmetry properties of $[ZnPc(-3)]^-$ and $[ZnPc(-4)]^-$ are similar, it should be possible to use the band assignment that has been developed for the optical spectra of $[MPc(-3)]^-$ to assign the major bands of the absorption and MCD spectra of the $[MPc(-4)]^{2-}$ species. Significant differences will be seen in the Q and B1 transitions of $[ZnPc(-3)]^-$ and $[ZnPc(-4)]^{2-}$, as electrons from lower orbitals cannot enter the filled b_{2g}* orbital of the Jahn−Teller split LUMO of $[ZnPc(-4)]^{2-}$, Figure 9. As the intensity mechanism for MCD B terms depends upon the degree of field-induced mixing of close lying states,[52] the MCD band arising from these transitions will be very weak, unless there is mixing with a state that arises from another transition. The absorption band at 805 nm (865 nm at 90 K) can, therefore, be assigned to the Q transition, as there is no corresponding MCD signal in this region of the spectrum, Figure 4. The ZINDO calculation significantly overestimates the energy of the Q band, Table 4, and as a result, significant mixing with the lowest energy $\pi^* \rightarrow \pi^*$ excited states is predicted.

The pair of coupled B terms at 506 and 620 nm, Figure 4, can be assigned to the $\pi^* \rightarrow \pi^*$ transition. As the $1a_u$* and $1b_{1u}$* orbitals are both empty, only two spin allowed excited state configurations are possible. The field-induced mixing between these states gives rise to the intense pair of coupled, oppositely-signed B terms, which dominates the MCD spectrum in this region. It is clear from the absorption spectrum that the origin of the bands in this spectral region is more complex than a simple pair of coupled transitions. The absorption band at 540 nm (534 nm at 90 K) is significantly more intense than the shoulder at 643 nm (624 nm at 90 K). Evidence of $n \rightarrow \pi^*$ transitions has been found in this region of the spectra of both $ZnPc(-2)$[25] and $[ZnPc(-3)]^-$.[13] In the 300−450 nm region, the second $\pi \rightarrow \pi^*$ and B1 excited states can couple with each other and to other higher energy states, and as a result, significant MCD intensity is seen.[26] The ZINDO calculation predicts that the second $\pi \rightarrow \pi^*$ transition will be the only $\pi \rightarrow \pi^*$ transition to give rise to significant intensity in this portion of the spectrum. The calculation also suggests that there may be two additional sets of weaker oppositely-signed B terms arising primarily from higher energy $\pi^* \rightarrow \pi^*$ transitions in this region. It is relatively easy to assign the bands in the calculated spectrum of $[ZnPc(-4)]^{2-}$, Table 4, to specific one-electron transitions as the symmetry is D_{2h}(II). The parity properties of the molecular orbitals greatly reduce the number of transitions which can contribute significant intensity to the major spectral bands.

Detailed analysis of the room and low-temperature absorption and MCD spectra of $ZnPc(-2)$[25] and $[ZnPc(-3)]^-$ [13] has indicated that the room temperature absorption spectral envelope is significantly broadened relative to the MCD spectral envelope due to the different selection rules associated with the two techniques. There is a significant red shift in the band centers of many of the major absorption bands of $[ZnPc(-3)]^-$ relative to those of the MCD spectrum, due to "hot bands" which arise from the population of vibrational levels associated with the ground state.[13] The MCD signal associated with the higher energy solvation environments is quenched as the orbital angular momentum of the excited states is reduced. The MCD band centers show a better agreement with the 90 K absorption spectrum as the absorption signal of the major transitions sharpens and blue shifts since the higher energy solvation environments are frozen out when the solution is vitrified. The major bands in the $\pi \rightarrow \pi^*$ region of the MCD spectrum are significantly broader than the corresponding bands in the spectrum of $[ZnPc(-3)]^-$, Figure 3. This is probably a result of the greater uncertainty associated with the radiative lifetimes of the excited states.[52]

The $[MPc(-5)]^{3-}$ Species. EPR evidence is consistent with a ground state containing a single-unpaired electron.[37,40] The ZINDO calculation places the unpaired electron in the lower energy orbital of the Jahn−Teller split LUMO, Table 5 (see Supporting Information), so no meaningful data could be obtained from the calculated absorption spectrum. The calculated orbitals did however show the same C_{2v}(III) symmetry[49]

(52) Hochstrasser, R. M.; Marzzacco, C. *J. Phys. Chem.* **1968**, *49*, 971.

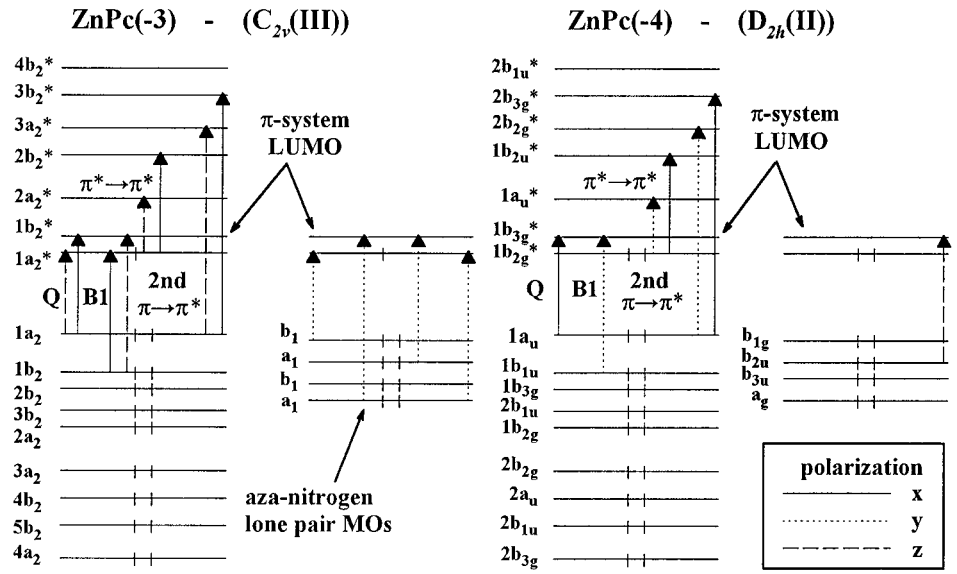

Figure 7. Molecular orbital diagrams for the π-system and aza-nitrogen lone pair orbitals of $[ZnPc(-3)]^-$ and $[ZnPc(-4)]^{2-}$, assuming C_{2v}(III) and D_{2h}(II) symmetry, respectively. The orbital ordering on the left is based on the results of our ZINDO calculation, Tables 3 and 4.

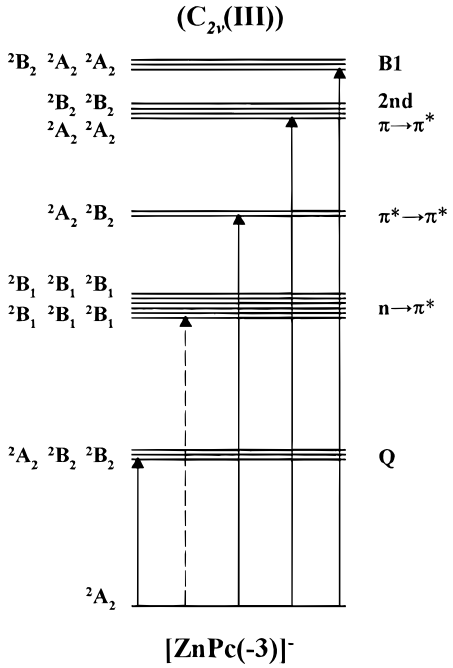

Figure 8. State energy level diagram of $[ZnPc(-3)]^-$, assuming C_{2v}-(III) symmetry. Transitions that give rise to *x*- or *z*-polarized bands are represented with solid lines. Dashed lines are used for *y*-polarized transitions. The n → π^* transitions are placed between the Q_{vib} and B1 transitions on the basis of the assignment of the Q region of (CN)-ZnPc(−2).[25]

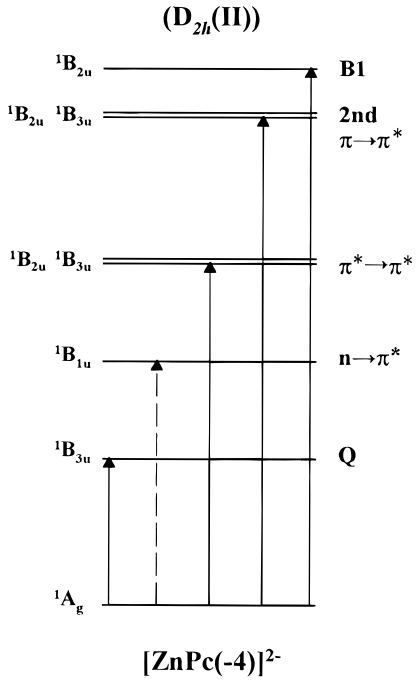

Figure 9. State energy level diagram of $[ZnPc(-4)]^{2-}$, assuming D_{2h}-(II) symmetry. Transitions that give rise to *x*- or *y*-polarized bands are represented with solid lines. Dashed lines are used for *z*-polarized transitions. The n → π^* transition is placed between the Q_{vib} and B1 transitions on the basis of the assignment of the Q region of (CN)-ZnPc(−2).[25]

that was seen with $[ZnPc(-3)]^-$, Figure 10. An initial band at 1125 nm in the spectrum of $[MgPc(-5)]^{3-}$ is assigned to the Q transition, Table 7.[3,11] Although the quality of Linder's absorption spectrum is low, the band appears to be a simple Gaussian curve and is not followed by any vibrational bands.[11] The occupation of both the $1a_2$* and $1b_2$* orbitals can be expected to lead to two separate sets of $\pi^* \rightarrow \pi^*$ bands, Figures 10 and 11. The broad absorption bands at 589 and 825 nm[3,11] are assigned to these transitions. The assumption is made that individual *x*- and *z*-polarized bands cannot be resolved in the absorption spectrum due to the band-broadening effects that were seen in the $\pi^* \rightarrow \pi^*$ region of the $[ZnPc(-4)]^{2-}$ spectrum. A band at 338 nm is assigned to the second $\pi \rightarrow \pi^*$ transition.[3,11] As the $1a_2$* orbital is fully occupied, two spin-allowed excited state configurations will be possible for the second $\pi \rightarrow \pi^*$ and the $\pi^* \rightarrow \pi^*$ transition, out of the $1a_2$ orbital, Figure 11.

The $[MPc(-6)]^{4-}$ Species. As would be expected, EPR measurements have indicated that the ground states of main group $[MPc(-6)]^{4-}$ species are diamagnetic,[37,40] as the LUMO of the neutral species is now fully populated, Figures 10 and 12. Our ZINDO calculation suggests that the fully occupied $1e_g$* orbital is almost degenerate, Table 6 (see Supporting Information), and that D_{4h} symmetry is essentially maintained.[49] As a result, the major transitions should give rise to ^1E_u excited states similar to those associated with the ZnPc(−2) and $[ZnPc(-1)]^+$ species. The absorption spectrum of $[MgPc(-6)]^{4-}$ reported by Linder *et al.*[11] is dominated by two intense

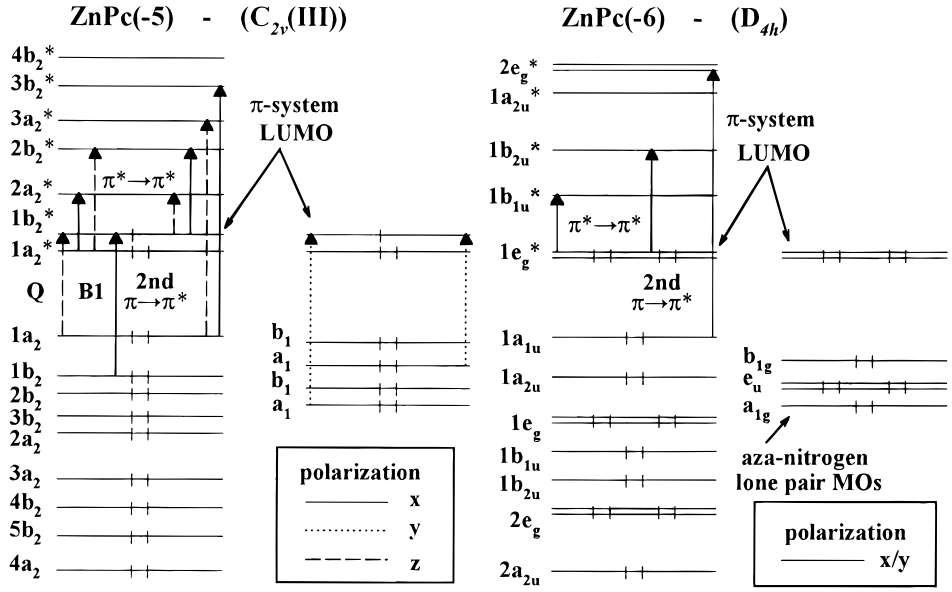

Figure 10. Molecular orbital diagrams for the π-system and aza-nitrogen lone pair orbitals of $[ZnPc(-5)]^{3-}$ and $[ZnPc(-6)]^{4-}$, assuming C_{2v}(III) and D_{4h} symmetry respectively. The orbital ordering on the left is based on the results of our ZINDO calculation, Tables 5 and 6 (see Supporting Information).

absorption bands at 625 and 840 nm. As the LUMO ±5 level is fully occupied, the near-IR−visible region of the spectrum can be expected to be dominated by the two $\pi^* \rightarrow \pi^*$ transitions from the $1e_g^*$ orbital to the symmetry-split $1b_{1u}^*$ and $1b_{2u}^*$ orbitals, Figure 10. Linder *et al.*[11] report an MCD signal for the 840 nm band which could be interpreted as a broad A term. The absorption spectrum of $[MgPc(-6)]^{4-}$ contains an additional intense band in the UV region, which can be assigned to the second $\pi \rightarrow \pi^*$ transition, Table 7, although our ZINDO calculation suggests that most of the absorption intensity in this region actually arises from a series of close lying higher energy $\pi^* \rightarrow \pi^*$ transitions.

Other MPc Complexes. The assignment of the spectra of main group phthalocyanines, such as MgPc and ZnPc, provides characteristic marker bands for the ring-reduced $[MPc(-3)]^-$, $[MPc(-4)]^{2-}$, $[MPc(-5)]^{3-}$, and $[MPc(-6)]^{4-}$ species that can be used to assign the more complex spectra of transition metal phthalocyanine anions where reduction of the metal is also possible. The spectra of the ZnPc and MgPc species are found to be almost identical.[18b] Table 7 contains a new assignment of the major bands for the ring-reduced anions of the metal phthalocyanines that were summarized by Clack and Yandle.[3] A number of these species conform well with the assignments presented already. Thus, the assignment of the spectral bands of the anion radical species of ring-reduced AlClPc, CoPc, and NiPc is relatively straightforward. The assignment of the CoPc anions is also reasonably straightforward, despite the fact that five anion species have been reported. The initial reduction product is assigned to a metal-reduced $[Co^{I}Pc(-2)]^-$ species.[53] The other four reduction products are in close agreement with four reduced species of main group metal phthalocyanine anions with an additional charge transfer band at around 476 nm (21 000 cm^{-1}), so the species are assigned to $[Co^{I}Pc(-(n+2))]^{(n+1)-}$ $(n = 1-4)$ species.

In contrast, the spectra of the anion species of FePc and MnPc are much more complicated. The exact nature of the FePc anions has not been fully established. The first reduced species of FePc was assigned by Clack and Yandle[3] to a ring-reduced $[Fe^{II}Pc(-1)]^-$ species but Lever and Wilshire[10] have subsequently shown that the EPR spectrum is more consistent with a metal-reduced $[Fe^{I}Pc(-2)]^-$ species. The optical data, Table 7, supports Lever's assignment as the λ_{max} values are clearly not consistent with a ring-reduced main group $[M(II)Pc(-3)]^-$ species. The second reduction product was assigned by Lever and Wilshire[10] to a $[Fe^{I}Pc(-3)]^-$ species on the basis of electrochemical evidence. As Clack and Yandle pointed out, the optical data appear to be more consistent with a $[Fe^{II}Pc(-4)]^{2-}$ species, so Clack's original assignment is used in Table 7. The correct formulation cannot be distinguished by EPR, as both species would be expected to adopt diamagnetic ground states.[10] The optical spectra of the third and fourth reduction products are similar to those of the main group $[MPc(-4)]^{2-}$ and $[MPc(-5)]^{3-}$ species and are thus assigned to $[Fe^{I}Pc(-4)]^{3-}$ and $[Fe^{I}Pc(-5)]^{4-}$, Table 7.

There is considerable doubt as to whether the first two reduction products of $Mn^{II}Pc$ are ring or metal reduced. The optical spectrum of the second reduction products reported for chemical reduction over sodium in THF[3] is clearly different from that reported for a hydrazine reduction of tetrasulfonated MnPc (MntsPc) in aqueous solution.[54] EPR evidence suggests that the hydrazine reduction product is $[Mn^{0}tsPc(-2)]^{2-}$,[54] while the optical spectrum of the sodium reduction product appears to be consistent with a $[Mn^{II}Pc(-4)]^{2-}$ species.[3] As no EPR signal was found for the $[MntsPc]^-$ species formed through a sodium sulfide reduction in aqueous solution, the species was assigned to $[Mn^{I}tsPc(-2)]^-$.[54] No optical spectra were reported. The optical spectrum of the first reduction product formed by sodium reduction is consistent with $[Mn^{II}Pc(-3)]^-$, although the Q transition appears to shift to higher energy and there appears to be an intense charge transfer band at 527 nm. We have, therefore, assigned this species to $[Mn^{II}Pc(-3)]^-$ in Table 7. This assignment cannot be regarded as definitive, however, as the separation of the first and second reduction processes appears to be significantly larger than that in other $MPc(-2)$ species,[55] while a more normal separation was found at elevated

(53) Stillman, M. J.; Thomson, A. J. *J. Chem. Soc., Faraday Trans. 2* **1974**, *70*, 790.

(54) Cookson, D. J.; Smith, T. D.; Boas, J. F.; Hicks, P. R.; Pilbrow, J. R. *J. Chem. Soc., Dalton Trans.* **1977**, 211.

(55) Lever, A. B. P.; Milaeva, E. R.; Speier, G. In *Phthalocyanine. Principles and Properties*; Leznoff, C. C., Lever A. B. P., Eds.; VCH Publications: New York, 1992; Vol. III, Chapter 1, pp 1−70.

Table 7. Band Assignments of Anion Species of Various Metal Phthalocyanine Complexes[a–c]

	[ZnPc(−3)]$^{-}$	[ZnPc(−4)]$^{2-}$	[ZnPc(−5)]$^{3-}$	[ZnPc(−6)]$^{4-}$
Q	10 550	12 950	9090	
$\pi^* \rightarrow \pi^*$ ($1b_2^*$)			...	12 180
$\pi^* \rightarrow \pi^*$ ($1a_2^*$)	15 720/17 790	19 160	17 540	16 130
second $\pi \rightarrow \pi^*$	24 270	29 850	29 410	32 890
B1	30 960	...	...	
ref	13	3	3	3
	[MgPc(−3)]$^{-}$	[MgPc(−4)]$^{2-}$	[MgPc(−5)]$^{3-}$	[MgPc(−6)]$^{4-}$
Q	10 420	11 110	8970	
$\pi^* \rightarrow \pi^*$ ($1b_2^*$)			12 120	11 910
$\pi^* \rightarrow \pi^*$ ($1a_2^*$)	15 670/17 790	19 230	16 950	16 130
second $\pi \rightarrow \pi^*$	23 810	29 850	29 500	32 790
B1	29 410	...	...	
ref	3	3	3	3
	[AlClPc(−3)]$^{-}$	[AlClPc(−4)]$^{2-}$	[AlClPc(−5)]$^{3-}$	[AlClPc(−6)]$^{4-}$
Q	10 260	11 110	9620	
$\pi^* \rightarrow \pi^*$ ($1b_2^*$)			12 500	12 350
$\pi^* \rightarrow \pi^*$ ($1a_2^*$)	13 810/17 390	19 230	19 310	16 560
second $\pi \rightarrow \pi^*$	...	29 850	30 580	28 990
B1	30 400	...	...	
ref	3	3	3	3
	[NiPc(−3)]$^{-}$	[NiPc(−4)]$^{2-}$	[NiPc(−5)]$^{3-}$	[NiPc(−6)]$^{4-}$
Q	10 930	10 990	9220	
$\pi^* \rightarrow \pi^*$ ($1b_2^*$)			11 240	11 360
$\pi^* \rightarrow \pi^*$ ($1a_2^*$)	15 870/17 790	18 660	16 950	14 880
second $\pi \rightarrow \pi^*$	24 040	30 030	30 000	32 150
B1	30 030	...	...	
ref	3	3	3	3
	[MnPc(−3)]$^{-}$	[MnPc(−4)]$^{2-}$	[MnPc(−5)]$^{3-}$	[MnPc(−6)]$^{4-}$
Q	11 980	14 120	9090	
$\pi^* \rightarrow \pi^*$ ($1b_2^*$)			12 020	...
$\pi^* \rightarrow \pi^*$ ($1a_2^*$)	15 870/17 240	19 160	17 670	16 130
CT	19 530	19 160	...	...
second $\pi \rightarrow \pi^*$	28 250	30 210	29 410	27 030
B1	30 400	...	...	
ref	3	3	3	3

	[Co^{I}Pc(−2)]$^{-}$	[Co^{I}Pc(−3)]$^{2-}$	[Co^{I}Pc(−4)]$^{3-}$	[Co^{I}Pc(−5)]$^{4-}$	[Co^{I}Pc(−6)]$^{5-}$
Q	14 410	10 870	8480/11 050	10 000	
$\pi^* \rightarrow \pi^*$ ($1b_2^*$)				11 490	11 300
$\pi^* \rightarrow \pi^*$ ($1a_2^*$)		14 680/16 000	19 160	17 670	14 490
CT	21 410	21 010	19 160	23 700	18 520
second $\pi \rightarrow \pi^*$	...	31 350	30 670	29 410	28 010
B1	32 050	...	...	...	
ref	3	3	3	3	3
	[Fe^{I}Pc(−2)]$^{-}$	[Fe^{II}Pc(−4)]$^{2-}$	[Fe^{I}Pc(−4)]$^{3-}$	[Fe^{I}Pc(−5)]$^{4-}$	
CT	12 500				
Q	15 040	13 510	...	7300	
$\pi^* \rightarrow \pi^*$ ($1b_2^*$)				13 020	
$\pi^* \rightarrow \pi^*$ ($1a_2^*$)		19 760	18 870	16 640	
CT	16 780/19 420	25 320	26 810	27 320	
second $\pi \rightarrow \pi^*$	...	29 410	29 590	...	
B1	30 670	...	...	...	
ref	3,10	3	3	3	

[a] λ_{max} (cm^{-1}) values for the major spectral bands in the electronic absorption spectra. [b] The central metal oxidation state is assigned as II in all of the Zn, Mg, AlCl, Ni, and Mn species included in this table. [c] The anion species were generated in ref 3 by chemical reduction *in vacuo* over sodium in THF, in ref 10 by electrochemical reduction in pyridine under nitrogen using LiCl as the supporting electrolyte, and in ref 13 by photochemical reduction in a DMF/hydrazine hydrate solvent mixture.

temperatures in a noncoordinating solvent.[56] The optical spectra and redox properties of the third and fourth reduction products formed by sodium reduction are consistent with the formation of [Mn^{II}Pc(−5)]$^{3-}$ and [Mn^{II}Pc(−6)]$^{4-}$ species.[3] The optical spectroscopy of ring- and metal-reduced MnPc and FePc anion species is an area that will require more detailed study before definitive band assignments can be made.

The band assignment scheme in Table 7 should greatly facilitate the assignment of absorption spectral data reported for the reduced species of the peripherally substituted phthalocyanine anions in the literature,[4–9] as peripheral substitution tends to have only a very minor impact on the spectral properties of the cyclic polyene π-system. The [MPc(−3)]$^{-}$ and [MPc(−4)]$^{2-}$ species reported in the literature show the characteristic marker bands for these species. A good example of this is the spectral data reported by Golovin *et al.* for the [$ZnCl_{16}$Pc(−

(56) Campbell, R. H.; Heath, G. A.; Hefter, G. T.; McQueen, R. C. S. *J. Chem. Soc., Chem. Commun.* **1983**, 1123.

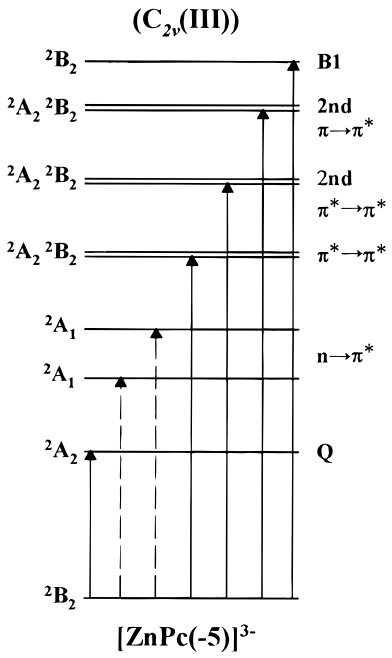

Figure 11. State energy level diagram of $[ZnPc(-5)]^{3-}$, assuming C_{2v}-(III) symmetry. Transitions that give rise to *x*- or *z*-polarized bands are represented with solid lines. Dashed lines are used for *y*-polarized transitions. The n → π^* transitions are placed between the Q_{vib} and B1 transitions on the basis of the assignment of the Q region of (CN)-ZnPc(−2).[25]

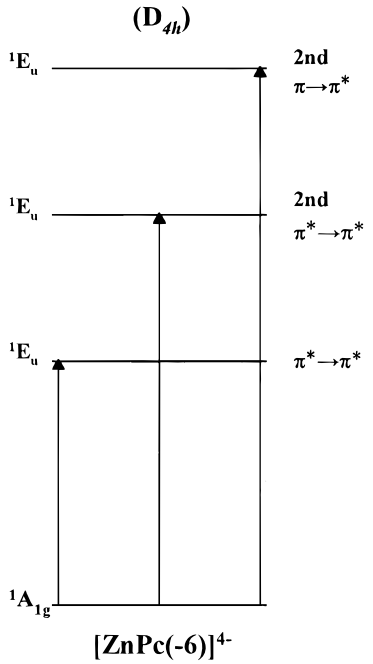

Figure 12. State energy level diagram of $[ZnPc(-6)]^{4-}$, assuming D_{4h} symmetry. Transitions that give rise to *x*/*y*-polarized bands are represented with solid lines.

3)]$^-$ and $[ZnCl_{16}Pc(-4)]^{2-}$ anion radicals,[9] which are almost identical to the spectra reported for $[ZnPc(-3)]^-$ and $[ZnPc(-4)]^{2-}$ in this paper.

Discussion

By measuring absorption and MCD spectral data for the main group $MPc(-2)$,[18,22−25] $[MPc(-3)]^-$,[13,28] and $[MPc(-4)]^{2-}$ species and using the data of Linder[11] for $[MPc(-5)]^{3-}$ and $[MPc(-6)]^{4-}$ together with the absorption data of Clack and Yandle,[3] we have been able to propose a unified assignment of the optical spectra of the anion species. As the same set of $\pi \rightarrow \pi^*$, $\pi \rightarrow \pi$, and $\pi^* \rightarrow \pi^*$ transitions give rise to bands in the neutral, ring-oxidized cation, and ring-reduced anion species of main group metal phthalocyanines, we can compare, Figure 13, the relative energies of the major transitions of each species by plotting the energies of the band centers against the number of electrons added or removed from the MgPc ring. Although transitions linking the lone pair orbitals of the aza-nitrogen lone pairs and the π-system can also be expected in the UV−vis region, these relatively weak n → π^* transitions cannot be identified easily in the more highly complex extensively overlapped MCD spectra of $[MPc(-(n + 2))]^{n-}$ ($n = 1-3$) species, as the more intense transitions of the π-system give rise to Gaussian-shaped B terms rather than the distinctive derivative-shaped A terms seen in the spectra of main group metal neutral and cationic species.

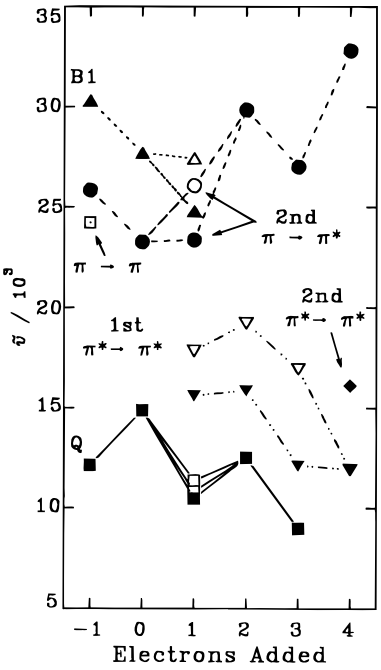

Figure 13. Relative energies of the major electronic transitions of the π-system of MgPc upon ring oxidation and reduction observed experimentally.[3,18,28] Different line types and symbols are used to link the bands of each major transition. Solid and hollow symbols are used to indicate excited states that are associated with oppositely-signed, coupled B terms in species subject to a static Jahn−Teller distortion.

Figure 13 provides strong evidence that the band assignment that we developed for $[ZnPc(-3)]^-$ [13] is valid, as the energy separations between the transitions in the different species are found to be consistent. Although the one-electron energy differences between the orbitals would normally be expected to be one of the most important factors determining the energies of the transitions, this has not been demonstrated previously over such a wide range of metal phthalocyanine redox states. The other major trend that can be seen in Figure 13 is that the energies of the major $\pi \rightarrow \pi^*$, $\pi \rightarrow \pi$, and $\pi^* \rightarrow \pi^*$ bands of species with diamagnetic ground states are higher than the comparable transitions for those with paramagnetic ground states. This is probably due to significant differences that may result from the two-electron Coulomb and exchange integrals between the electrons in species with paramagnetic ground states. There is also a slight trend to lower energy in the Q band as electrons are added to the π-system, which suggests that the gap between the $1a_{1u}$ and $1e_g^*$ orbitals narrows as electrons are added to the Jahn−Teller split LUMO.

It should be remembered, however, that significant configuration interaction takes place between close lying excited states,

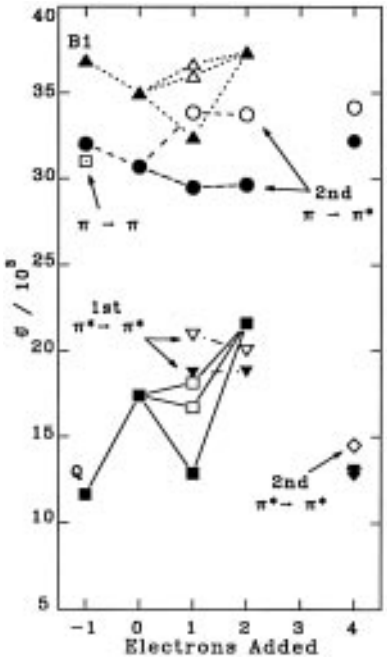

Figure 14. Relative energies of the pure electronic configurations of the major electronic transitions of the π-system of ZnPc upon ring oxidation and reduction that are predicted by the ZINDO program of the CAChe molecular modeling system. Different line types and symbols are used to link the bands of each major transition. Solid and hollow symbols are used to indicate excited states associated with oppositely-signed, coupled B terms in species subject to a static Jahn−Teller distortion.

so the one-electron transitions identified in Figure 13 only represent a first-order assignment. Our ZINDO calculations indicate that configuration interaction is particularly significant in the case of species with paramagnetic ground states so that several one-electron transitions contribute significantly to the higher energy transitions. As the MCD spectral data in the Q region of $[ZnPc(-3)]^-$ provides direct spectral evidence that the ZINDO calculation does not satisfactorily account for the static Jahn−Teller distortion of the ground state of $[ZnPc(-3)]^-$, it seems unwise to attempt to draw detailed conclusions from the analysis of the configuration interaction calculations for the $[ZnPc(-3)]^-$ and $[ZnPc(-4)]^{2-}$ species. The agreement between our assignment of the available experimental dats, Figure 14, and the energies of the pure one-electron transitions predicted by the ZINDO program is remarkably strong, however, and provides further evidence for the validity of our assignment scheme.

Conclusions

MCD spectroscopy has provided the essential additional information that was required to develop a detailed assignment of the complex overlapping absorption spectra of metal phthalocyanine anion species. The absence of A and C terms in the MCD spectra of $[MgPc(-3)]^-$ and $[ZnPc(-3)]^-$ represented the first direct spectral evidence that the orbital degeneracies of both the ground and excited states are lifted upon ring reduction. A band assignment for the major *x*- and *z*-polarized transitions has been developed, which is based upon the band polarization information obtained from the oppositely-signed coupled B terms in a band deconvolution analysis of $[ZnPc(-3)]^-$. This assignment has been extended successfully to the spectra of the more highly reduced $[MPc(-4)]^{2-}$, $[MPc(-5)]^{3-}$, and $[MPc(-6)]^{4-}$ species. A general assignment of the major transitions associated with the π-system of the phthalocyanine ring in six different redox states can therefore now be made. The assignments have been modified to reflect the results of MO calculations using the ZINDO program on $[MPc(-(n+2))]^{n-}$ $(n = -1-4)$ species. The assignment reported in Figure 13 should be of great benefit to theoretical chemists in developing improved models of the electronic structure of the phthalocyanine ring in the future.

Acknowledgment. We thank the Province of Ontario and the University of Western Ontario (UWO) for a differential fee waiver (to J.M.) and the NSERC of Canada for Operating and Equipment grants (to M.J.S.). M.J.S. is a member of the Centre for Chemical Physics and the Photochemistry Unit at UWO. This is publication 528 of the Photochemical Unit at UWO.

Supporting Information Available: Tables 5 and 6, which provide the calculated MO energies for $[ZnPc(-5)]^{3-}$ and $[ZnPc(-6)]^{4-}$ from the ZINDO program (3 pages). Ordering information is given on any current masthead page.

IC960737I